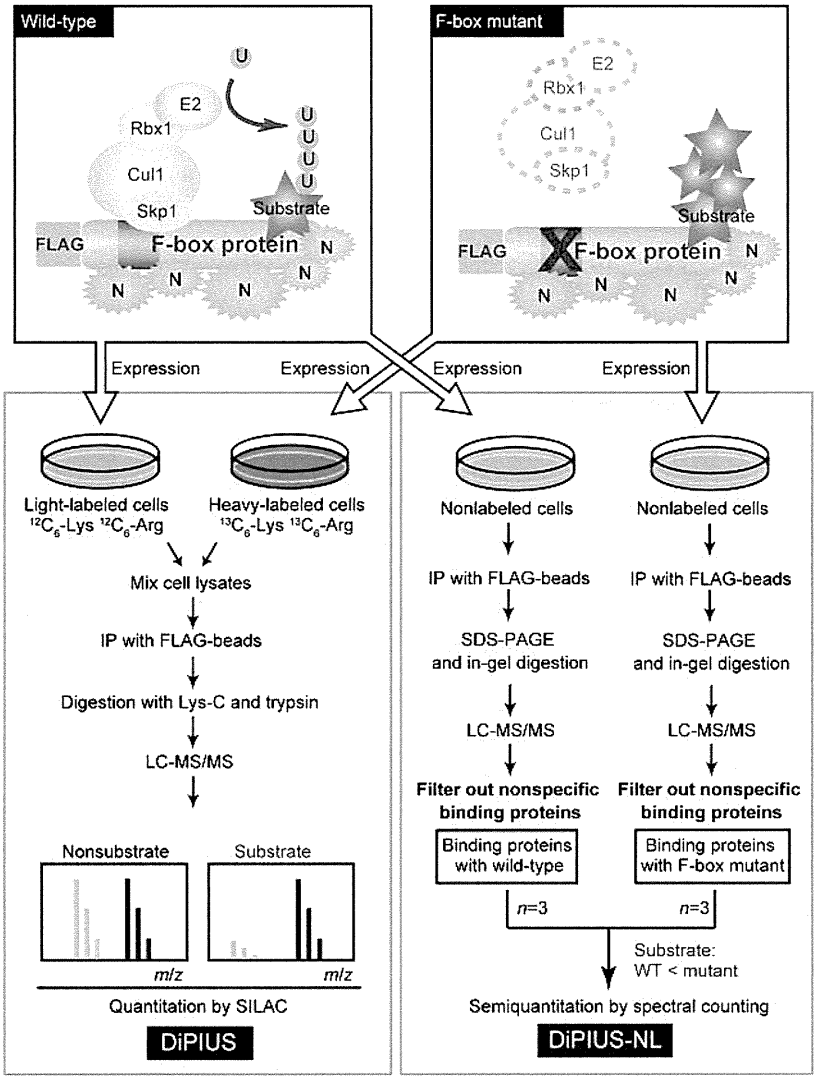

Figure 2. Strategy for comprehensive identification of substrates for an F-box protein. Schematic representations of DiPIUS and DiPIUS-NL are shown. Proteins that bind to WT or mutant F-box proteins are analyzed by quantitative SILAC (DiPIUS) or semiquantitative spectral counting (DiPIUS-NL). U, ubiquitin; N, nonspecific binding protein.

cell. We thus expected that whereas wild-type F-box proteins interact transiently with their substrates, mutant F-box proteins might stably associate with such substrates as the concentration of the latter would be increased. On the other hand, proteins that bind nonspecifically to other proteins would be expected to associate with wild-type and mutant F-box proteins to similar extents. To validate this hypothesis, we examined the interactions of Fbxw7α and Skp2 (also known as Fbxl1), two of the most well-characterized F-box proteins, with their representative substrates c-Myc and p27, respectively, as positive controls. We designed mutant Fbxw7α and Skp2 proteins that are unable to associate with the Cul1-Rbx1 module. In the case of Fbxw7α, the entire F-box domain was deleted (ΔF mutant), given that such deletion does not compromise binding to substrates. The COOH-terminal tail of Skp2 loops back to the F-box domain;[24] therefore, a large deletion within the F-box domain might be expected to affect the structure of the substrate-binding region, which is composed of many leucine-rich repeats. We thus replaced only two amino acids (P113 and E115) in the F-box domain that are essential for the association of Skp2 with Cul1 with alanine (PE/AA mutant).[14,25] As expected, coimmunoprecipitation analysis revealed that FLAG epitope-tagged wild-type Fbxw7α bound weakly to endogenous c-Myc, whereas more c-Myc was associated with the FLAG-tagged Fbxw7$\alpha(\Delta F)$ mutant (Figure 1A). Likewise, FLAG-tagged wild-type Skp2 associated weakly with endogenous p27, whereas the FLAG-tagged Skp2(PE/AA) mutant interacted with p27 to a greater extent (Figure 1B).

To isolate comprehensively the proteins that associate with mutant F-box proteins more efficiently than with wild-type F-box proteins, we developed the DiPIUS system (Figure 2). Wild-type or mutant forms of F-box proteins tagged at their NH_2 termini with the FLAG epitope were expressed in mCAT-HeLa or HEK293T cells and subjected to SILAC analysis.[26] Cells expressing the wild-type protein were cultured in regular (light) medium, whereas those expressing the mutant protein were cultured in medium containing stable isotope-labeled amino acids (heavy medium). Cell lysates were mixed and subjected to immunoprecipitation with antibodies to FLAG, and tryptic digests of the immunoprecipitates were analyzed by liquid chromatography and tandem MS (LC-MS/MS) (Figure 3 and Tables S1 and S2 in the Supporting Information). Alternatively, tryptic digests of immunoprecipitates derived

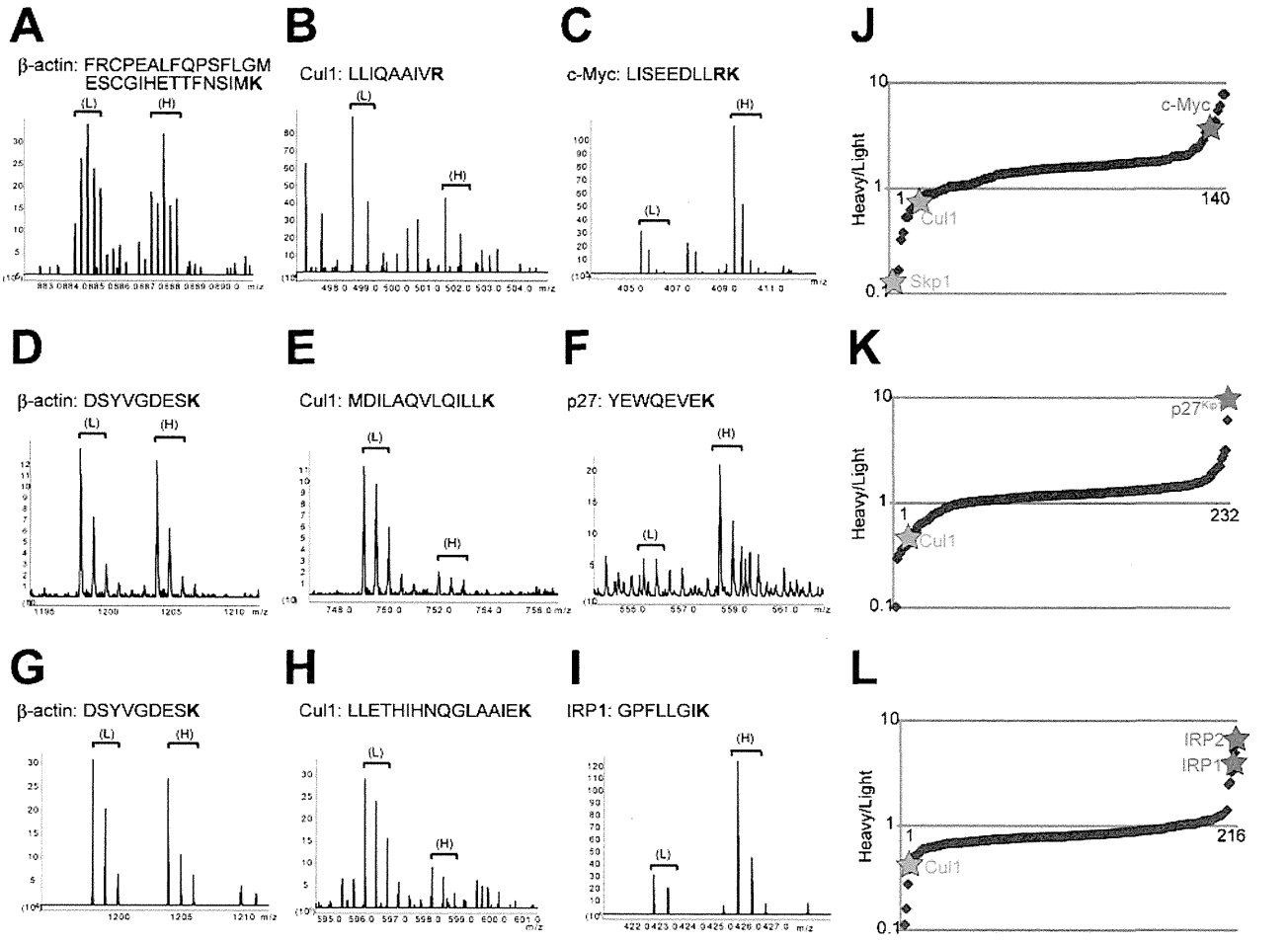

Figure 3. Candidate substrates for Fbxw7α, Skp2, and Fbxl5 analyzed by quantitative SILAC. (A–I) Representative mass spectra of SILAC analyses. Peak areas of light (L) and heavy (H) tryptic peptides derived from β-actin (A), Cul1 (B), or c-Myc (C) represent the abundance of proteins associated with WT and mutant Fbxw7α, respectively; those from β-actin (D), Cul1 (E), or p27 (F) represent the abundance of proteins associated with WT and mutant Skp2, respectively; and those from β-actin (G), Cul1 (H), or IRP1 (I) represent the abundance of proteins associated with WT and mutant Fbxl5, respectively. (J–L) Plot diagrams of heavy/light ratios for SILAC analysis of Fbxw7α (J), Skp2 (K), and Fbxl5 (L).

separately from lysates of nonlabeled cells expressing the wild-type or mutant F-box proteins were subjected to semi-quantitative spectral counting, a nonlabeling method hereafter referred to as DiPIUS-NL (Figure 4).

Identification of Candidate Substrates for F-box Proteins by DiPIUS

We applied DiPIUS to Fbxw7α, Skp2, and Fbxl5, three of the most well-characterized F-box proteins. SILAC ratios of proteins were normalized by the heavy/light ratio for each bait protein. We set the threshold for candidate substrates as a heavy/light ratio of $\geq$3 on the basis of the measurement of experimental error when equal amounts (1:1) of heavy- and light-labeled samples prepared from the same mCAT-HeLa cells expressing FLAG-tagged wild-type Skp2 were subjected to immunoprecipitation and analyzed; all of the detected proteins were included within the range of the ratio from 0.5 to 2.0 (Figure S1 in the Supporting Information). DiPIUS is based on the assumption that the expression levels of wild-type and mutant F-box proteins are identical. These levels are not perfectly identical in most cases, however, with small differences resulting in a slight shift in the baseline of the heavy/light ratio.

We identified many candidate proteins including previously known substrates such as c-Myc for Fbxw7α[9,10] (Figure 3C,J), p27 for Skp2[9,11] (Figure 3F,K), and IRP1 and IRP2 for Fbxl5[27,28] (Figure 3I,L). These substrates yielded almost the highest scores of SILAC analysis (heavy/light ratio) among the binding proteins. In contrast, β-actin, a representative non-specific protein, was found in almost equal amounts in the immunoprecipitates containing the wild-type or mutant F-box proteins (Figure 3A,D,G). Cul1, a component of SCF ubiquitin ligases, showed low scores on SILAC analysis in all experiments (Figure 3B,E,H), indicating that the mutant form of each F-box protein was unable to form a complete SCF complex. These results thus validated DiPIUS as a means to identify substrates for F-box proteins.

Given that only a few substrates for Fbxw7α, Skp2, and Fbxl5 were identified by the original DiPIUS system with SILAC, these F-box proteins were also subjected to DiPIUS-NL with spectral counting. With this approach, we identified from three independent experiments a total of 426, 379, and 515 proteins that associated with Fbxw7α, Skp2, and Fbxl5, respectively (Figure 4A and Tables S3 and S4 in the Supporting Information). Among these binding molecules, 405, 362, and 418 proteins, respectively, were eliminated because they were identified as proteins that interact with at least two of Fbxw7α, Skp2, and Fbxl5. The remaining 21, 17, and 97 proteins, respectively, were subjected to a more detailed analysis of the

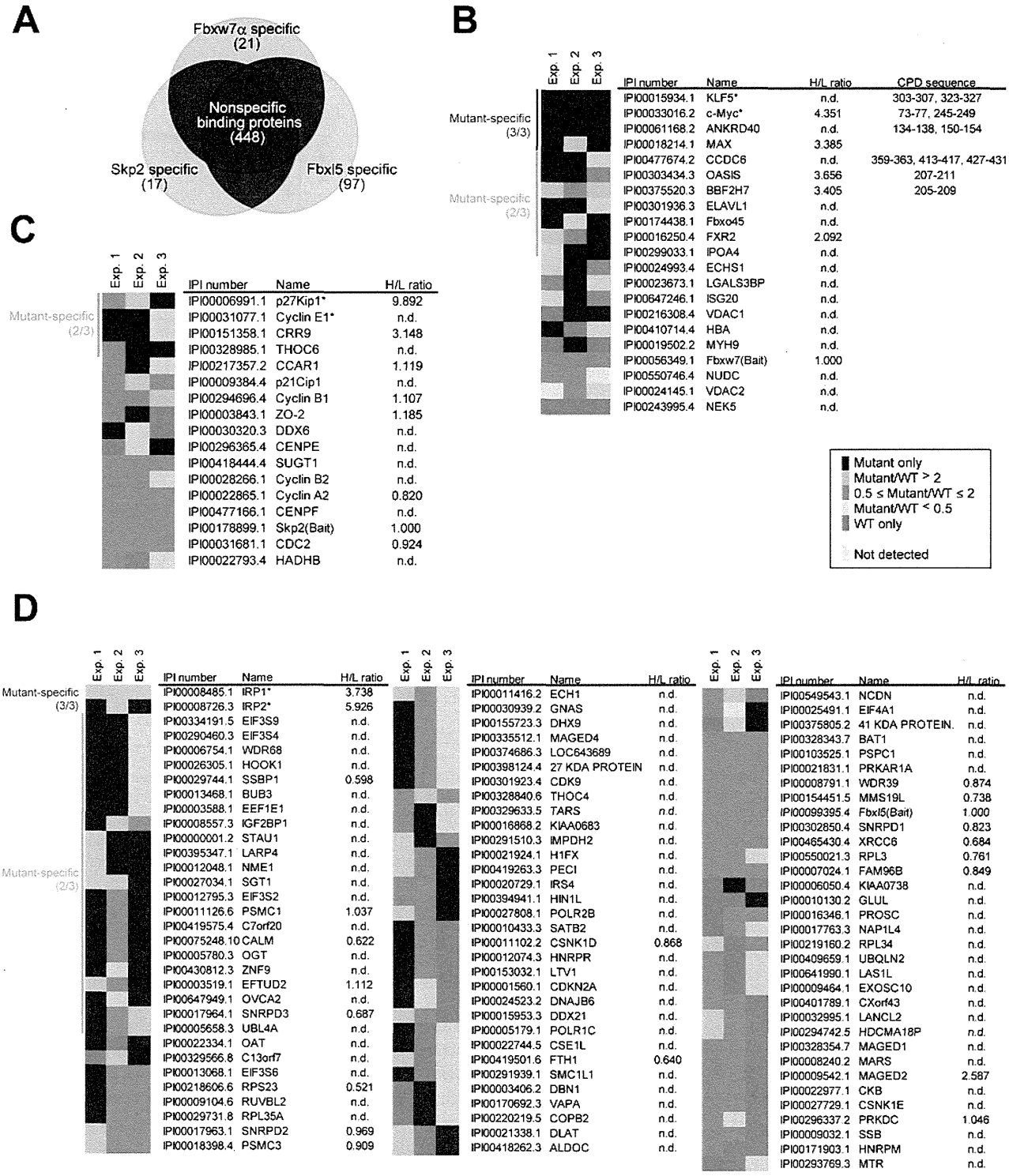

Figure 4. Candidate substrates for Fbxw7α, Skp2, and Fbxl5 analyzed by semiquantitative spectral counting. (A) Venn diagram for identified binding proteins for each F-box protein. (B–D) Specific binding proteins for Fbxw7α (B), Skp2 (C), and Fbxl5 (D) are shown. The ratios of the number of spectral counts for WT and mutant F-box proteins are indicated by the color scale. Proteins with a mutant/WT ratio of >2 in at least two of three independent experiments (Exp.) were considered binding proteins that associate to a greater extent with the mutant F-box protein than with the WT protein. The mutant (heavy)/WT (light) SILAC ratios (H/L ratios) obtained by original DiPIUS analysis are also shown. Proteins that contain a CPD sequence are indicated in (B). n.d., not detected. Asterisks indicate known substrates.

ratio of the spectral counts for the wild-type and mutant F-box proteins (spectral count score) in the individual experiments. We set the threshold as a score of >2 in at least two of three independent experiments for candidate substrates that preferentially bind to the mutant F-box protein. About 4.2% of proteins were classified as false positives at this threshold on the basis of the measurement of experimental error with mCAT-HeLa cells expressing wild-type Skp2 (Figure S2 in the Supporting Information). c-Myc was identified as a substrate for Fbxw7α (Figure 4B), consistent with our previous

observation that ablation of c-Myc reversed the overproliferation phenotype of Fbxw7-deficient thymocytes.[29] In addition, the transcription factor Krüppel-like factor 5 (KLF5), another known substrate for Fbxw7α,[30,31] yielded the highest score. For Skp2, both p27 and cyclin E1 were identified as candidate substrates (Figure 4C), consistent with previous observations.[32,33] IRP1 and IRP2 were identified as substrates for Fbxl5 with the highest scores (Figure 4D), consistent with the results of the original DiPIUS method (Figure 3L) as well as with our previous genetic data showing that IRP2 is the major substrate of Fbxl5 and that ablation of IRP2 prevents the embryonic death of Fbxl5-deficient mice.[34] SSBP1, PSMC1, CALM, EFTUD2, and SNRPD3 were also detected as candidate substrates of Fbxl5 by semiquantitative DiPIUS-NL, even though these proteins had a low heavy/light ratio in SILAC analysis (Figure 4D). DiPIUS-NL is therefore able to detect a wider spectrum of candidate substrates for F-box proteins but also yields more pseudopositive results compared with the original DiPIUS system with SILAC.

Among the 21 proteins remaining after elimination of 405 multibinders from the 426 total proteins that associated with Fbxw7α, 10 proteins were categorized as candidate substrates (score of >2) by DiPIUS-NL analysis. Six of these 10 proteins (60%) contain a consensus sequence for Fbxw7 binding, known as the Cdc4 phosphodegron (CPD) (Figure 5). In contrast,

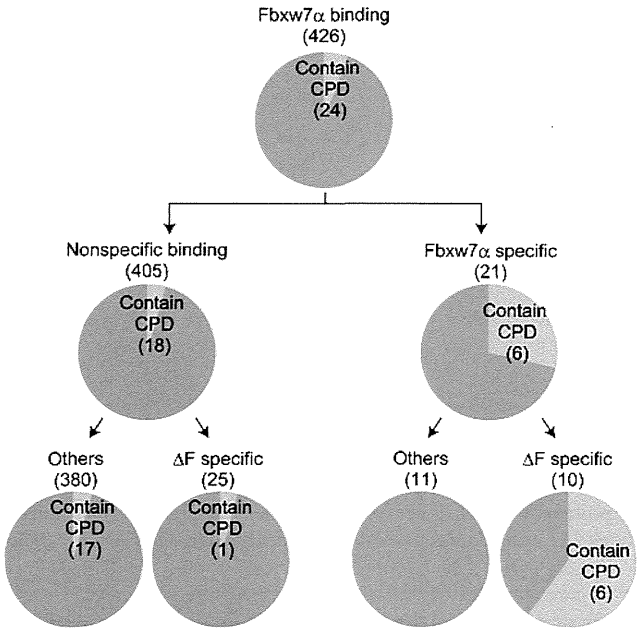

Figure 5. Number and distribution of Fbxw7α binding proteins in DiPIUS-NL analysis. Binding proteins for Fbxw7α were divided into two groups: "nonspecific binders", which also bound to Skp2 or Fbxl5 (or both), and "Fbxw7α-specific binders". The binding proteins were also classified as ΔF mutant-specific binders or not. Proteins that contain a CPD sequence are enriched among Fbxw7α(ΔF)-specific binders.

among the 405 nonspecific binders to Fbxw7α, 25 proteins were found to have a spectral count score of >2. However, only one (4%) of these 25 proteins contains the CPD sequence. These results suggest that elimination of the proteins that interact with multiple F-box proteins is effective for enrichment of real substrates. Proteins that do not contain the CPD sequence but which bound to the mutant form of Fbxw7α may thus represent false positives. For example, MAX, a binding partner of c-Myc, was detected by this approach as a false positive, probably because c-Myc preferentially associated with the Fbxw7α mutant. Together, these results suggested that DiPIUS is effective for the identification of the substrates of F-box proteins.

Enrichment Analysis of Specific Binding Proteins for F-box Proteins

We categorized the proteins identified by DiPIUS-NL as specific binding proteins for Fbxw7α, Skp2, or Fbxl5 with the use of the DAVID resource to highlight the most over-represented Gene Ontology (GO) annotation terms (>2-fold enrichment as compared with a *Homo sapiens* background; $P < 0.05$) for molecular functions (Figure 6A) or biological processes (Figure 6B). Such enrichment analysis revealed that the molecular function of "transcription factor activity" was significantly enriched (>4-fold) for the Fbxw7α-specific binding proteins (Figure 6A), consistent with the fact that known substrates for Fbxw7α including c-Myc, Notch, KLF5, c-Jun, TGIF, and SREBP are all classified in this category. These results suggested that Fbxw7α preferentially targets transcriptional factors for degradation. With regard to biological processes, the categories of "positive regulation of cellular process" and "catabolic process" were also enriched for Fbxw7α-specific binding proteins (Figure 6B). For the Skp2-specific binding proteins, the biological processes of "cell division", "cell cycle process", and "cell cycle" showed a >10-fold enrichment as compared with the general human background (Figure 6B), suggesting that Skp2 specifically associates with cell cycle regulators. This finding is also consistent with the fact that Skp2 targets the Cip/Kip family of cyclin-dependent kinase inhibitors (p21, p27, and p57) and G_1 cyclins (cyclins D1 and E1) for ubiquitylation.[9,11] For the Fbxl5-specific binding proteins, no annotation terms showed an enrichment of more than 3-fold (Figure 6). Together, these results suggested that some F-box proteins are specialized for specific cellular and molecular functions.

Identification of Different Sets of Substrates in Different Cell Types or under Different Conditions

Although many substrates have been previously identified for Fbxw7 and Skp2, only a subset of these substrates was identified by DiPIUS in mCAT-HeLa cells. We expected that if any of the substrates, corresponding kinases, or signaling molecules that activate the kinases are lacking in HeLa cells, then these substrates would not be detected by DiPIUS. To verify this assumption, we applied DiPIUS-NL to Fbxw7α in mouse cell lines including mHepa (hepatocyte cell line), Neuro2A (neuroblastoma cell line), and C2C12 (mesenchymal cell line). We identified other known substrates for Fbxw7α, including TGIF1, TGIF2, SREBP1, SREBP2, and c-Myb, in mHepa, Neuro2A, or C2C12 cells (Figure 7A and Table S5 in the Supporting Information), with none of these proteins having been identified in mCAT-HeLa cells. Whereas c-Myc was identified in all cell lines tested, KLF5 was detected by DiPIUS-NL only in mCAT-HeLa and C2C12 cells. c-Myb was identified only in Neuro2A cells.

We also applied DiPIUS-NL to Skp2 in mHepa and C2C12 cells, the latter of which were cultured under either growth- or differentiation-promoting conditions (Figure 7B and Tables S6 and S7 in the Supporting Information). Although p27 was detected in all cell lines tested, the spectrum of identified substrates differed substantially among mCAT-HeLa, mHepa,

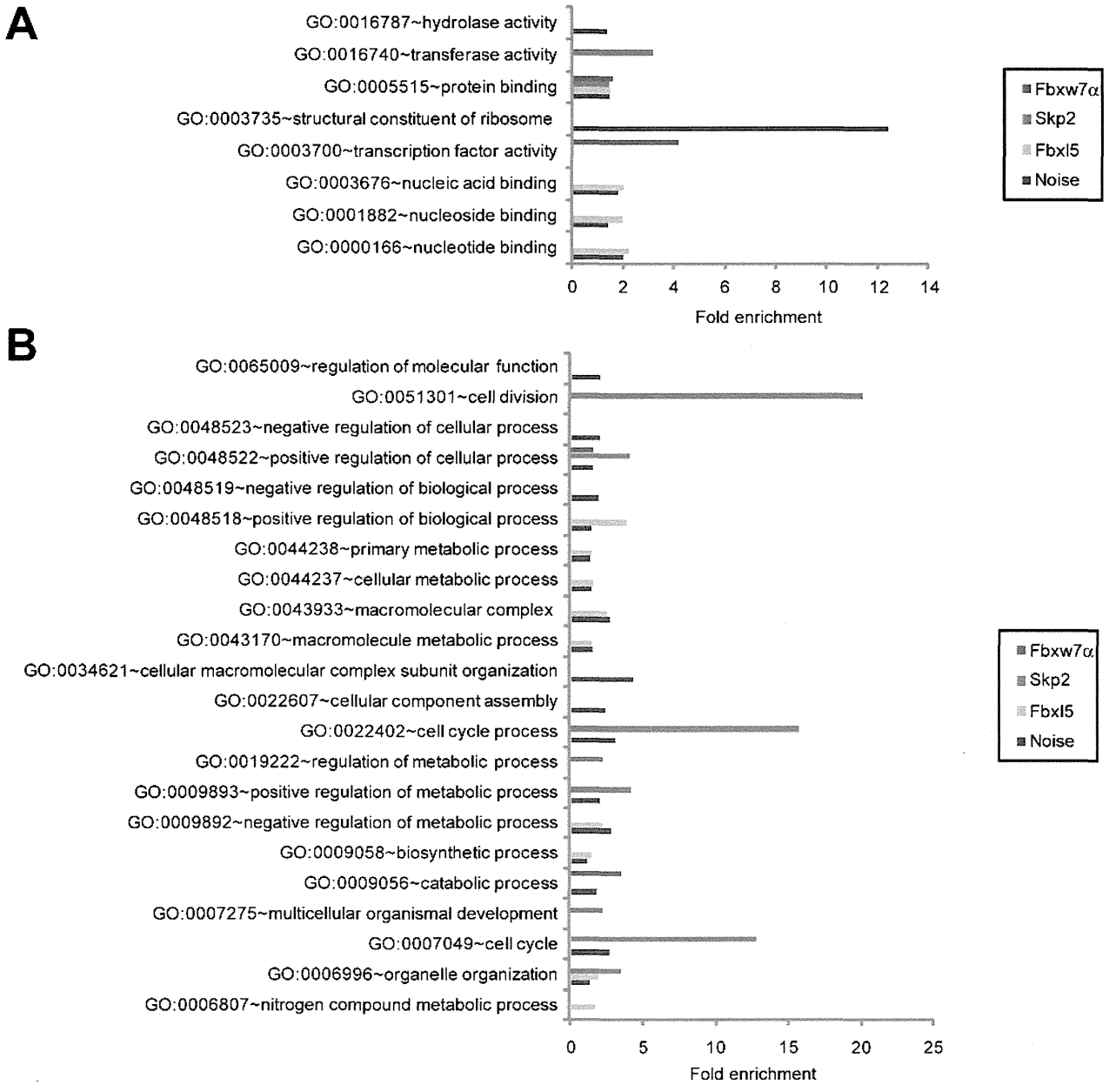

Figure 6. Functional analysis of differentially enriched proteins among binding proteins for each F-box protein. Fold enrichment among binding proteins for Fbxw7α, Skp2, or Fbxl5 of GO categories related to molecular functions (A) or biological processes (B) identified by DAVID ($P < 0.05$) are shown.

and C2C12 cells. Furthermore, cyclin E1, Cks1, Kif23, cyclin D3, Rnf12, and Mprip were identified as candidate substrates in C2C12 cells only under the growth condition, whereas Mypt1 and Gadd45α were identified as candidate substrates in these cells only under the differentiation (myoblast) condition. These results thus suggest that different sets of substrates are identified in different cell types or under different conditions by DiPIUS.

DISCUSSION

We have shown here that the DiPIUS approach identifies multiple substrates of a ubiquitin ligase in a comprehensive and unbiased manner. Several approaches to the identification of the substrates for mammalian ubiquitin ligases have been described.[35−37] However, there are several advantages of DiPIUS over such conventional methods that depend on simple purification of the substrates on the basis of their affinity for a given ubiquitin ligase. The principle of DiPIUS is based on a difference in the abundance of substrates between cells expressing wild-type or mutant F-box proteins. The many nonspecific proteins that are usually most problematic in conventional methods are efficiently eliminated by the DiPIUS system, given that such nonspecific proteins are expected to bind to wild-type and mutant F-box proteins to a similar extent. Our approach thus concentrates candidate substrates by eliminating many nonspecific proteins.

Most importantly, DiPIUS is applicable to any F-box protein. In addition to the SCF complex, DiPIUS has proved effective for the identification of substrates for the elongin B/C−Cul2−VHL-box protein (ECV) complex; we thus identified hypoxia-inducible factors (HIFs) as substrates of VHL[38,39] by DiPIUS (K. Y., M. M., and K. I. N., unpublished results). These

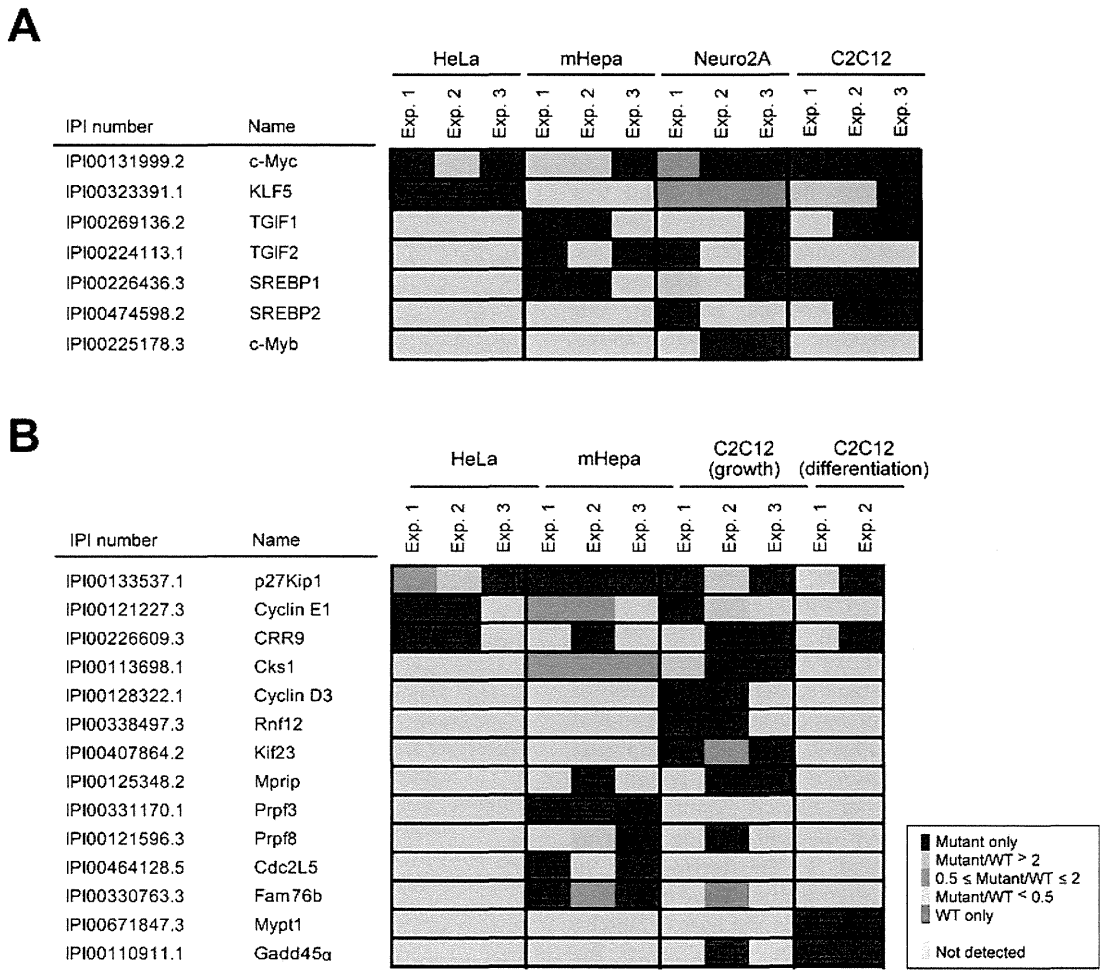

Figure 7. Known substrates of Fbxw7α and Skp2 analyzed by DiPIUS-NL in different cell types or under different conditions. (A) Known substrates for Fbxw7α detected by DiPIUS-NL in mCAT-HeLa (same as in Figure 4B), mHepa, Neuro2A, and C2C12 cells. The ratios of the number of spectral counts for WT and mutant F-box proteins are indicated by the color scale. Proteins with a mutant/WT ratio of >2 in at least two of three independent experiments (Exp.) were considered binding proteins that associate with the mutant F-box protein to a greater extent than with the WT protein. (B) Known and candidate substrates for Skp2 detected by DiPIUS-NL in mCAT-HeLa cells (same as in Figure 4C), mHepa cells, and C2C12 cells (cultured under growth- or myoblast differentiation-promoting conditions).

preliminary results suggest that DiPIUS may be applicable to all classes of cullin-based ubiquitin ligases. Moreover, in principle, DiPIUS could be applied to any ubiquitin ligase. A limitation of DiPIUS, which is based on protein degradation, is that it is unable to identify substrates for which ubiquitylation does not serve as a signal for degradation. DiPIUS appears to be highly sensitive, given that its application to F-box proteins has identified many low-abundance proteins including transcription factors. In addition, the number of cells required for DiPIUS is relatively small; we used 4×10^7 mCAT-HeLa cells per DiPIUS experiment. Furthermore, nonspecific binding proteins that usually render the discovery of bona fide substrates difficult in interaction-based technologies are efficiently removed by the comparison of protein profiles between wild-type and mutant ubiquitin ligases.

We have described two alternative forms of the DiPIUS system: original DiPIUS with SILAC and DiPIUS-NL with semiquantitative spectral counting. Original DiPIUS is effective for quantitation of the abundance of binding proteins for wild-type and mutant F-box proteins, although the number of such proteins identified is smaller than that detected by DiPIUS-NL. This latter problem is likely attributable to a greater complexity of the samples used for original DiPIUS as compared with those used for DiPIUS-NL; lysates of light isotope- and heavy isotope-labeled cells corresponding to proteins bound to wild-type and mutant F-box proteins, respectively, are thus mixed in original DiPIUS, and the immunoprecipitates derived therefrom are digested and analyzed directly without fractionation by SDS-PAGE and in-gel digestion. Although SDS-PAGE and in-gel digestion may reduce the complexity of samples, however, the increased processing may result in sample loss and a consequent reduction in both signal intensity and quantitative capacity. Furthermore, whereas the reduced sample complexity in DiPIUS-NL results in an increase in the number of candidate substrates identified, it also inevitably gives rise to a substantial number of false positives (~4.2%). We therefore propose that the two DiPIUS methods are complementary and should both be applied to obtain more comprehensive and precise results. Candidates identified by DiPIUS-NL analysis can be eliminated if their quantitation by original DiPIUS does not yield a high heavy/light score. Validation studies are necessary to verify that the candidates identified by DiPIUS-NL are indeed substrates of the ubiquitin ligase of interest.

Given that many substrates have been previously identified for Fbxw7 and Skp2, it was unexpected that only a subset of these substrates was identified by DiPIUS. There are several

possible explanations for this outcome. First, ubiquitylation requires that various conditions be satisfied, including that the substrate, ubiquitin ligase, corresponding kinase, and signals to activate the kinase be present in a cell (or a limited compartment of the cell) at the same time. The performance of DiPIUS in different cell types might thus be expected to identify different sets of substrates. Indeed, we found that different sets of substrates for Fbxw7α or Skp2 were discovered by DiPIUS in different cell types or under different conditions. Second, the sensitivity of DiPIUS might not be high enough for the detection of low-abundance proteins. However, this possibility seems unlikely given that, as mentioned above, DiPIUS identified many transcription factors that are expressed at a low level. Third, ubiquitylation of some of the proteins that were designated substrates on the basis of previous results might occur infrequently in the physiological setting. Consistent with this notion, some of these putative substrates were found not to accumulate in mice or cells that lack Skp2.[9,11]

As mentioned above, the application of DiPIUS to different cell types led to the identification of different substrates. These observations appear consistent with our previous genetic analyses of mice in which the Fbxw7 gene is conditionally ablated in a variety of tissues. Distinct subsets of substrates for Fbxw7 accumulate in such mutant mice in a tissue-dependent manner. For example, loss of Fbxw7 in the hematopoietic system results in c-Myc accumulation that leads to lymphomagenesis.[29,40] Hepatic ablation of *Fbxw7* results in the accumulation of sterol regulatory element-binding proteins (SREBPs) and Notch1, which leads to the development of steatohepatitis and hamartoma, whereas the abundance of c-Myc is not affected by the loss of Fbxw7 in the liver.[41] Notch1 accumulates in the Fbxw7-deficient brain, which affects the maintenance of neural stem cells,[42] whereas the abundance of c-Myc and SREBPs in the brain is not increased in this mutant during embryogenesis. Collectively, our biochemical and genetic studies suggest that a given ubiquitin ligase targets a different set of substrates in each cell or tissue type.

Comprehensive identification of substrates for a given ubiquitin ligase may provide valuable clues to the physiological functions of the enzyme. The DiPIUS system will thus likely provide important insight into the functions of ubiquitin ligases, the number of genes for which is estimated to be >500 in the human genome.[7]

■ ASSOCIATED CONTENT

Supporting Information

Supplementary Figures S1 and S2 and Tables S1–S7. This material is available free of charge via the Internet at http://pubs.acs.org.

■ AUTHOR INFORMATION

Corresponding Author

*Tel: +81-92-642-6815. Fax: +81-92-642-6819. E-mail: nakayak1@bioreg.kyushu-u.ac.jp.

Notes

The authors declare no competing financial interest.

■ ACKNOWLEDGMENTS

We thank T. Kitamura for pMX-puro; J. M. Cunningham and K. Hanada for the mCAT-1 plasmid; M. Oda, E. Koba, N. Nishimura, T. Takami, and other laboratory members for technical assistance; and M. Kimura and A. Ohta for help with preparation of the manuscript. This work was supported in part by a grant from the Ministry of Education, Culture, Sports, Science, and Technology of Japan.

■ REFERENCES

(1) Payen, A.; Persoz, J. F. Memoire sur la Diastase, les Principaux Produits de ses Reactions, et leurs Applications aux arts Industriels. *Ann. Chim. (Phys.)* **1833**, *53*, 73–92.

(2) Lohmann, K. Über die enzymatische Aufspaltung der Kreatinphosphorsäure; zugleich ein Beitrag zum Chemismus der Muskelkontraktion. *Biochem. Z* **1934**, *271*, 264–277.

(3) Irniger, S.; Piatti, S.; Michaelis, C.; Nasmyth, K. Genes involved in sister chromatid separation are needed for B-type cyclin proteolysis in budding yeast. *Cell* **1995**, *81* (2), 269–278.

(4) King, R. W.; Peters, J. M.; Tugendreich, S.; Rolfe, M.; Hieter, P.; Kirschner, M. W. A 20S complex containing CDC27 and CDC16 catalyzes the mitosis-specific conjugation of ubiquitin to cyclin B. *Cell* **1995**, *81* (2), 279–288.

(5) Sudakin, V.; Ganoth, D.; Dahan, A.; Heller, H.; Hershko, J.; Luca, F. C.; Ruderman, J. V.; Hershko, A. The cyclosome, a large complex containing cyclin-selective ubiquitin ligase activity, targets cyclins for destruction at the end of mitosis. *Mol. Biol. Cell* **1995**, *6* (2), 185–197.

(6) Manning, G.; Whyte, D. B.; Martinez, R.; Hunter, T.; Sudarsanam, S. The protein kinase complement of the human genome. *Science* **2002**, *298* (5600), 1912–1934.

(7) Semple, C. A. The comparative proteomics of ubiquitination in mouse. *Genome Res.* **2003**, *13* (6B), 1389–1394.

(8) Hershko, A.; Ciechanover, A. The ubiquitin system. *Annu. Rev. Biochem.* **1998**, *67*, 425–479.

(9) Nakayama, K. I.; Nakayama, K. Ubiquitin ligases: Cell-cycle control and cancer. *Nat. Rev. Cancer* **2006**, *6* (5), 369–381.

(10) Welcker, M.; Clurman, B. E. FBW7 ubiquitin ligase: a tumour suppressor at the crossroads of cell division, growth and differentiation. *Nat. Rev. Cancer* **2008**, *8* (2), 83–93.

(11) Frescas, D.; Pagano, M. Deregulated proteolysis by the F-box proteins SKP2 and β-TrCP: Tipping the scales of cancer. *Nat. Rev. Cancer* **2008**, *8* (6), 438–449.

(12) Jin, J.; Cardozo, T.; Lovering, R. C.; Elledge, S. J.; Pagano, M.; Harper, J. W. Systematic analysis and nomenclature of mammalian F-box proteins. *Genes Dev.* **2004**, *18* (21), 2573–2580.

(13) Liao, E. H.; Hung, W.; Abrams, B.; Zhen, M. An SCF-like ubiquitin ligase complex that controls presynaptic differentiation. *Nature* **2004**, *430* (6997), 345–350.

(14) Saiga, T.; Fukuda, T.; Matsumoto, M.; Tada, H.; Okano, H. J.; Okano, H.; Nakayama, K. I. Fbxo45 forms a novel ubiquitin ligase complex and is required for neuronal development. *Mol. Cell. Biol.* **2009**, *29* (13), 3529–3543.

(15) Wolters, H.; Jurgens, G. Survival of the flexible: hormonal growth control and adaptation in plant development. *Nat. Rev. Genet.* **2009**, *10* (5), 305–317.

(16) Godinho, S. I.; Maywood, E. S.; Shaw, L.; Tucci, V.; Barnard, A. R.; Busino, L.; Pagano, M.; Kendall, R.; Quwailid, M. M.; Romero, M. R.; O'Neill, J.; Chesham, J. E.; Brooker, D.; Lalanne, Z.; Hastings, M. H.; Nolan, P. M. The after-hours mutant reveals a role for Fbxl3 in determining mammalian circadian period. *Science* **2007**, *316* (5826), 897–900.

(17) Siepka, S. M.; Yoo, S. H.; Park, J.; Song, W.; Kumar, V.; Hu, Y.; Lee, C.; Takahashi, J. S. Circadian mutant Overtime reveals F-box protein FBXL3 regulation of cryptochrome and period gene expression. *Cell* **2007**, *129* (5), 1011–1023.

(18) Busino, L.; Bassermann, F.; Maiolica, A.; Lee, C.; Nolan, P. M.; Godinho, S. I.; Draetta, G. F.; Pagano, M. SCF^{Fbxl3} controls the oscillation of the circadian clock by directing the degradation of cryptochrome proteins. *Science* **2007**, *316* (5826), 900–904.

(19) Albritton, L. M.; Tseng, L.; Scadden, D.; Cunningham, J. M. A putative murine ecotropic retrovirus receptor gene encodes a multiple

membrane-spanning protein and confers susceptibility to virus infection. *Cell* **1989**, *57* (4), 659–666.
(20) Matsumoto, M.; Hatakeyama, S.; Oyamada, K.; Oda, Y.; Nishimura, T.; Nakayama, K. I. Large-scale analysis of the human ubiquitin-related proteome. *Proteomics* **2005**, *5* (16), 4145–4151.
(21) Dennis, G., Jr.; Sherman, B. T.; Hosack, D. A.; Yang, J.; Gao, W.; Lane, H. C.; Lempicki, R. A. DAVID: Database for Annotation, Visualization, and Integrated Discovery. *Genome Biol.* **2003**, *4* (5), P3.
(22) Kitagawa, M.; Hatakeyama, S.; Shirane, M.; Matsumoto, M.; Ishida, N.; Hattori, K.; Nakamichi, I.; Kikuchi, A.; Nakayama, K.; Nakayama, K. An F-box protein, FWD1, mediates ubiquitin-dependent proteolysis of β-catenin. *EMBO J.* **1999**, *18* (9), 2401–2410.
(23) Kamura, T.; Hara, T.; Kotoshiba, S.; Yada, M.; Ishida, N.; Imaki, H.; Hatakeyama, S.; Nakayama, K.; Nakayama, K. I. Degradation of $p57^{Kip2}$ mediated by SCF^{Skp2}-dependent ubiquitylation. *Proc. Natl. Acad. Sci. U.S.A.* **2003**, *100* (18), 10231–10236.
(24) Schulman, B. A.; Carrano, A. C.; Jeffrey, P. D.; Bowen, Z.; Kinnucan, E. R.; Finnin, M. S.; Elledge, S. J.; Harper, J. W.; Pagano, M.; Pavletich, N. P. Insights into SCF ubiquitin ligases from the structure of the Skp1-Skp2 complex. *Nature* **2000**, *408* (6810), 381–386.
(25) Kamura, T.; Maenaka, K.; Kotoshiba, S.; Matsumoto, M.; Kohda, D.; Conaway, R. C.; Conaway, J. W.; Nakayama, K. I. VHL-box and SOCS-box domains determine binding specificity for Cul2-Rbx1 and Cul5-Rbx2 modules of ubiquitin ligases. *Genes Dev.* **2004**, *18* (24), 3055–3065.
(26) Ong, S. E.; Blagoev, B.; Kratchmarova, I.; Kristensen, D. B.; Steen, H.; Pandey, A.; Mann, M. Stable isotope labeling by amino acids in cell culture, SILAC, as a simple and accurate approach to expression proteomics. *Mol. Cell. Proteomics* **2002**, *1* (5), 376–386.
(27) Salahudeen, A. A.; Thompson, J. W.; Ruiz, J. C.; Ma, H. W.; Kinch, L. N.; Li, Q.; Grishin, N. V.; Bruick, R. K. An E3 ligase possessing an iron-responsive hemerythrin domain is a regulator of iron homeostasis. *Science* **2009**, *326* (5953), 722–726.
(28) Vashisht, A. A.; Zumbrennen, K. B.; Huang, X.; Powers, D. N.; Durazo, A.; Sun, D.; Bhaskaran, N.; Persson, A.; Uhlen, M.; Sangfelt, O.; Spruck, C.; Leibold, E. A.; Wohlschlegel, J. A. Control of iron homeostasis by an iron-regulated ubiquitin ligase. *Science* **2009**, *326* (5953), 718–721.
(29) Onoyama, I.; Tsunematsu, R.; Matsumoto, A.; Kimura, T.; de Alboran, I. M.; Nakayama, K.; Nakayama, K. I. Conditional inactivation of Fbxw7 impairs cell-cycle exit during T cell differentiation and results in lymphomatogenesis. *J. Exp. Med.* **2007**, *204* (12), 2875–2888.
(30) Liu, N.; Li, H.; Li, S.; Shen, M.; Xiao, N.; Chen, Y.; Wang, Y.; Wang, W.; Wang, R.; Wang, Q.; Sun, J.; Wang, P. The Fbw7/human CDC4 tumor suppressor targets proproliferative factor KLF5 for ubiquitination and degradation through multiple phosphodegron motifs. *J. Biol. Chem.* **2010**, *285* (24), 18858–18867.
(31) Zhao, D.; Zheng, H. Q.; Zhou, Z.; Chen, C. The Fbw7 tumor suppressor targets KLF5 for ubiquitin-mediated degradation and suppresses breast cell proliferation. *Cancer Res.* **2010**, *70* (11), 4728–4738.
(32) Nakayama, K.; Nagahama, H.; Minamishima, Y. A.; Matsumoto, M.; Nakamichi, I.; Kitagawa, K.; Shirane, M.; Tsunematsu, R.; Tsukiyama, T.; Ishida, N.; Kitagawa, M.; Nakayama, K. I.; Hatakeyama, S. Targeted disruption of *Skp2* results in accumulation of cyclin E and $p27^{Kip1}$, polyploidy and centrosome overduplication. *EMBO J.* **2000**, *19* (9), 2069–2081.
(33) Nakayama, K.; Nagahama, H.; Minamishima, Y. A.; Miyake, S.; Ishida, N.; Hatakeyama, S.; Kitagawa, M.; Iemura, S.; Natsume, T.; Nakayama, K. I. Skp2-mediated degradation of p27 regulates progression into mitosis. *Dev. Cell* **2004**, *6* (5), 661–672.
(34) Moroishi, T.; Nishiyama, M.; Takeda, Y.; Iwai, K.; Nakayama, K. I. The FBXL5-IRP2 axis is integral to control of iron metabolism in vivo. *Cell Metab.* **2011**, *14* (3), 339–351.
(35) Yen, H. C.; Elledge, S. J. Identification of SCF ubiquitin ligase substrates by global protein stability profiling. *Science* **2008**, *322* (5903), 923–929.
(36) Merbl, Y.; Kirschner, M. W. Large-scale detection of ubiquitination substrates using cell extracts and protein microarrays. *Proc. Natl. Acad. Sci. U.S.A.* **2009**, *106* (8), 2543–2548.
(37) Burande, C. F.; Heuze, M. L.; Lamsoul, I.; Monsarrat, B.; Uttenweiler-Joseph, S.; Lutz, P. G. A label-free quantitative proteomics strategy to identify E3 ubiquitin ligase substrates targeted to proteasome degradation. *Mol. Cell Proteomics* **2009**, *8* (7), 1719–1727.
(38) Jaakkola, P.; Mole, D. R.; Tian, Y. M.; Wilson, M. I.; Gielbert, J.; Gaskell, S. J.; Kriegsheim, A.; Hebestreit, H. F.; Mukherji, M.; Schofield, C. J.; Maxwell, P. H.; Pugh, C. W.; Ratcliffe, P. J. Targeting of HIF-α to the von Hippel-Lindau ubiquitylation complex by O_2-regulated prolyl hydroxylation. *Science* **2001**, *292* (5516), 468–472.
(39) Ivan, M.; Kondo, K.; Yang, H.; Kim, W.; Valiando, J.; Ohh, M.; Salic, A.; Asara, J. M.; Lane, W. S.; Kaelin, W. G., Jr. HIFα targeted for VHL-mediated destruction by proline hydroxylation: Implications for O_2 sensing. *Science* **2001**, *292* (5516), 464–468.
(40) Matsuoka, S.; Oike, Y.; Onoyama, I.; Iwama, A.; Arai, F.; Takubo, K.; Mashimo, Y.; Oguro, H.; Nitta, E.; Ito, K.; Miyamoto, K.; Yoshiwara, H.; Hosokawa, K.; Nakamura, Y.; Gomei, Y.; Iwasaki, H.; Hayashi, Y.; Matsuzaki, Y.; Nakayama, K.; Ikeda, Y.; Hata, A.; Chiba, S.; Nakayama, K. I.; Suda, T. Fbxw7 acts as a critical fail-safe against premature loss of hematopoietic stem cells and development of T-ALL. *Genes Dev.* **2008**, *22* (8), 986–991.
(41) Onoyama, I.; Suzuki, A.; Matsumoto, A.; Tomita, K.; Katagiri, H.; Oike, Y.; Nakayama, K.; Nakayama, K. I. Fbxw7 regulates lipid metabolism and cell fate decisions in the mouse liver. *J. Clin. Invest.* **2011**, *121* (1), 342–354.
(42) Matsumoto, A.; Onoyama, I.; Sunabori, T.; Kageyama, R.; Okano, H.; Nakayama, K. I. Fbxw7-dependent degradation of Notch is required for control of "stemness" and neuronal-glial differentiation in neural stem cells. *J. Biol. Chem.* **2011**, *286* (15), 13754–13764.

Cell

The Skp2-SCF E3 Ligase Regulates Akt Ubiquitination, Glycolysis, Herceptin Sensitivity, and Tumorigenesis

Chia-Hsin Chan,[1] Chien-Feng Li,[5,6,11] Wei-Lei Yang,[1,4] Yuan Gao,[1,4] Szu-Wei Lee,[1,4] Zizhen Feng,[1] Hsuan-Ying Huang,[7] Kelvin K.C. Tsai,[6] Leo G. Flores,[2] Yiping Shao,[3] John D. Hazle,[3] Dihua Yu,[1,4] Wenyi Wei,[8] Dos Sarbassov,[1,4] Mien-Chie Hung,[1,4,10] Keiichi I. Nakayama,[9] and Hui-Kuan Lin[1,4,*]

[1]Department of Molecular and Cellular Oncology
[2]Department of Experimental Diagnostic Imaging
[3]Department of Image Physics
The University of Texas MD Anderson Cancer Center, Houston, TX 77030, USA
[4]The University of Texas Graduate School of Biomedical Sciences at Houston, Houston, TX 77030, USA
[5]Department of Pathology, Chi-Mei Foundational Medical Center, Tainan 710, Taiwan
[6]National Institute of Cancer Research, National Health Research Institutes, Tainan 704, Taiwan
[7]Department of Pathology, Chang Gung Memorial Hospital-Kaohsiung Medical Center, Chang Gung University College of Medicine, Kaohsiung County 833, Taiwan
[8]Department of Pathology, Beth Israel Deaconess Medical Center, Harvard Medical School, Boston, MA 02215, USA
[9]Department of Molecular and Cellular Biology, Medical Institute of Bioregulation, Kyushu University, Fukuoka, Fukuoka 812-8582, Japan
[10]Center for Molecular Medicine and Graduate Institute of Cancer Biology, China Medical University and Hospital, Taichung 404, Taiwan
[11]Department of Biotechnology, Southern Taiwan University, Tainan 710, Taiwan
*Correspondence: hklin@mdanderson.org
DOI 10.1016/j.cell.2012.02.065

SUMMARY

Akt kinase plays a central role in cell growth, metabolism, and tumorigenesis. The TRAF6 E3 ligase orchestrates IGF-1-mediated Akt ubiquitination and activation. Here, we show that Akt ubiquitination is also induced by activation of ErbB receptors; unexpectedly, and in contrast to IGF-1 induced activation, the Skp2 SCF complex, not TRAF6, is a critical E3 ligase for ErbB-receptor-mediated Akt ubiquitination and membrane recruitment in response to EGF. Skp2 deficiency impairs Akt activation, Glut1 expression, glucose uptake and glycolysis, and breast cancer progression in various tumor models. Moreover, Skp2 overexpression correlates with Akt activation and breast cancer metastasis and serves as a marker for poor prognosis in Her2-positive patients. Finally, Skp2 silencing sensitizes Her2-overexpressing tumors to Herceptin treatment. Our study suggests that distinct E3 ligases are utilized by diverse growth factors for Akt activation and that targeting glycolysis sensitizes Her2-positive tumors to Herceptin treatment.

INTRODUCTION

Akt kinase is a key factor that conveys growth factor signals from outside the cell to inside the cell. It serves as a central node for the regulation of cell proliferation, cell survival, metabolism, and tumorigenesis (Brazil et al., 2002; Liu et al., 2009; Manning and Cantley, 2007; Yang et al., 2010a). The recruitment of Akt kinase to the plasma membrane is a critical step for Akt phosphorylation and activation by growth-factor stimuli. Although the PIP3 formation-induced by PI3K activation is essential for Akt membrane recruitment, our recent study reveals that K63-linked ubiquitination of Akt is also required for this process. TRAF6 is found to be an ubiquitin ligase (E3) for Akt and plays a crucial role in Akt ubiquitination, membrane translocation, and phosphorylation upon stimulation with insulin-like growth factor-1 (IGF-1) (Yang et al., 2009, 2010b). Thus, Akt ubiquitination and PIP3 binding are two important events required for Akt membrane recruitment and activation in response to IGF-1. However, it remains largely unclear whether Akt ubiquitination is universally engaged in Akt membrane translocation and activation triggered by other growth factor receptors, such as ErbB family.

Under normoxic condition, differentiated cells primarily utilize mitochondria oxidative phosphorylation to generate adenosine 5′-triphosphate (ATP) for biogenesis and cellular processes (Aragonés et al., 2009; Vander Heiden et al., 2009). However, under hypoxia these cells switch their metabolism from aerobic oxidative phosphorylation to anaerobic glycolysis. Notably, tumor cells utilize aerobic glycolysis regardless of the oxygen levels, known as the Warburg effect. The elevated aerobic glycolysis seen in tumor cells rapidly generates ATP in order to meet their increased need for energy and biosynthesis to sustain tumor growth (Birnbaum, 2004; Plas and Thompson, 2005; Robey and Hay, 2009). Akt kinase is frequently activated in various tumor types and represents one of the main drivers for the Warburg effect (Elstrom et al., 2004). Akt increases glucose

uptake by enhancing transcription and membrane translocation of glucose transporters. It promotes glycolytic flux through increasing hexokinase and phosphofructokinase activity (Robey and Hay, 2009). Accumulating evidence shows that the activation of the Akt pathway causes increased dependency on aerobic glycolysis (Elstrom et al., 2004; Wieman et al., 2007), suggesting that therapeutic strategies that target the Akt pathway can block glucose metabolism and consequently result in tumor regression. Although numerous downstream players involved in Akt-mediated glycolysis have been proposed, current knowledge regarding the upstream regulators of Akt-dependent glycolytic pathway remains limited.

In this study, we unexpectedly discover that Skp2, rather than TRAF6, is critically involved in ErbB family-induced Akt ubiquitination, aerobic glycolysis and tumorigenesis. Importantly, targeting glycolysis by Skp2 deficiency sensitizes Her2-positive tumors to Herceptin treatment, highlighting the clinical value of Skp2 targeting in breast cancer therapy.

RESULTS

Skp2 Is Responsible for EGF-Mediated Akt Ubiquitination

To determine whether Akt ubiquitination is a common event induced by growth factors, we examined whether Akt ubiquitination is induced by activation of epidermal growth factor (EGF) receptor, a member of the ErbB receptor family. Indeed, in vivo ubiquitination assay revealed that endogenous Akt ubiquitination is also induced upon EGF treatment (Figures 1A and 1E; Figure S1F, top, available online), suggesting that Akt ubiquitination is a general event triggered by growth factors. As TRAF6 is important for IGF-1-mediated Akt ubiquitination and activation (Yang et al., 2009), we determined whether EGF-mediated Akt ubiquitination and activation depend on TRAF6. To our surprise, EGF-induced ubiquitination of Akt and phosphorylation of Akt and Foxo1 were comparable between *WT* and *Traf6*$^{-/-}$ MEFs (Figures S1A and S1B), suggesting that TRAF6 is dispensable for EGF-induced Akt activation.

Skp2 is an F-Box protein that forms a Skp2 SCF complex with Skp1, Cullin-1 (Cul-1), and RBx1 to constitute an E3 ligase activity that triggers protein ubiquitination and degradation (Chan et al., 2010b; Nakayama and Nakayama, 2006). Skp2 displays oncogenic activities by regulating cell cycle progression, senescence, and metastasis (Chan et al., 2010a, 2011; Lin et al., 2009, 2010). As we have previously demonstrated that Akt physically interacts with Skp2 in vivo in response to IGF-1 (Lin et al., 2009), we determined whether Skp2 is engaged in EGF-mediated Akt ubiquitination. Although Akt ubiquitination upon EGF stimulation was induced in *WT* MEFs or control-knockdown cells, it was impaired in *Skp2*$^{-/-}$ MEFs and Skp2 knockdown cells (Figures 1A and 1E and S1F, top), indicating that Skp2 is required for EGF-induced Akt ubiquitination. Moreover, the interaction between endogenous Skp2 and Akt was also enhanced by EGF (Figures 1B and S1C), which occurred both in cytosol and nucleus (Figure S1D). Notably, Skp2 overexpression induced Akt ubiquitination in the absence of proteosome inhibitor, which did not cause Akt degradation (Figure 1C). Skp2 overexpression promoted lysine (K) 63-linked, rather than K48-linked, ubiquitination of Akt (Figure 1D). We further demonstrated that EGF markedly promoted endogenous K63-linked, rather than K48-linked, ubiquitination of Akt, which was diminished upon Skp2 deficiency (Figures 1E, S1E, and S1F). Although TRAF6 knockdown reduced the basal Akt ubiquitination and IGF-1-induced Akt phosphorylation and activation, Skp2 overexpression was still able to efficiently induce Akt ubiquitination (Figure S1G), suggesting that Skp2 promotes Akt ubiquitination independent of TRAF6.

Diverse Growth Factors Utilize Distinct E3 Ligase for Akt Ubiquitination and Activation

Although TRAF6 plays a critical role in IGF-1-mediated Akt ubiquitination and activation (Yang et al., 2009), this current study shows that EGF selectively utilizes the Skp2 SCF complex to ubiquitinate Akt. To gain further mechanistic insights into how ErbB and IGF-1 selectivity utilize distinct E3 ligases for Akt activation, we investigated the possibility that EGF and IGF-1 may do so by regulating their E3 ligase activities. Skp2, but not TRAF6, interacted with EGFR and its E3 ligase activity was enhanced upon EGF treatment, as judged by the formation of the Skp2 SCF complex (Figures 1F and S2A). In contrast, TRAF6 associated with IGF-1Rβ and its E3 ligase activity, as determined by TRAF6 auto-ubiquitination, was induced by IGF-1, but not by EGF stimulation (Figures 1G and S2B). Moreover, although IGF-1 readily activated TRAF6 within 15 min, it could not promote the formation of Skp2-SCF complex at this early time point, although it indeed does so after 1 hr (Figure S2C), consistent with our previous observation (Lin et al., 2009). Additionally, the endogenous expression of Skp2 was not affected by IGF-1 stimulation within 1 hr (Figure S2D). Thus, these results demonstrated that Skp2 is not activated at early time points, but it is activated at longer time points. Because IGF-1 induces the association of TRAF6 with Akt (Yang et al., 2009) and EGF stimulates the interaction between Skp2 and Akt (Figures 1B and S1C), we postulated that a potential mechanism responsible for this distinctive dependence on TRAF6 and Skp2 may be due to their different binding affinity for Akt. Indeed, we found that EGF selectively induced the interaction of Akt with Skp2, but not with TRAF6 (Figure S2E), providing an explanation of why Skp2, but not TRAF6, is involved in ErbB family-induced Akt ubiquitination.

Given that phosphorylation is a well-characterized posttranslational modification that regulates protein-protein interaction, we hypothesized that IGF-1 and EGF may regulate the interaction of Akt with Skp2 or TRAF6 by inducing their phosphorylation. In support of this notion, TRAF6 was tyrosine-, but not serine/threonine-, phosphorylated upon IGF-1 treatment (Figure S2F, upper and middle panels). In contrast, EGF failed to induce TRAF6 tyrosine phosphorylation (Figure S2F, lower panel). To further understand whether IGF-1-mediated TRAF6 phosphorylation may regulate TRAF6 and Akt interaction, we treated the TRAF6 immunocomplex with phosphatase to induce TRAF6 dephosphorylation and found that IGF-1-induced TRAF6 and Akt interaction was diminished (Figure S2G). Although Skp2 underwent tyrosine and serine/threonine phosphorylation upon EGF stimulation, the phosphatase treatment resulted in Skp2 dephosphorylation, accompanied by Skp2 and Akt dissociation

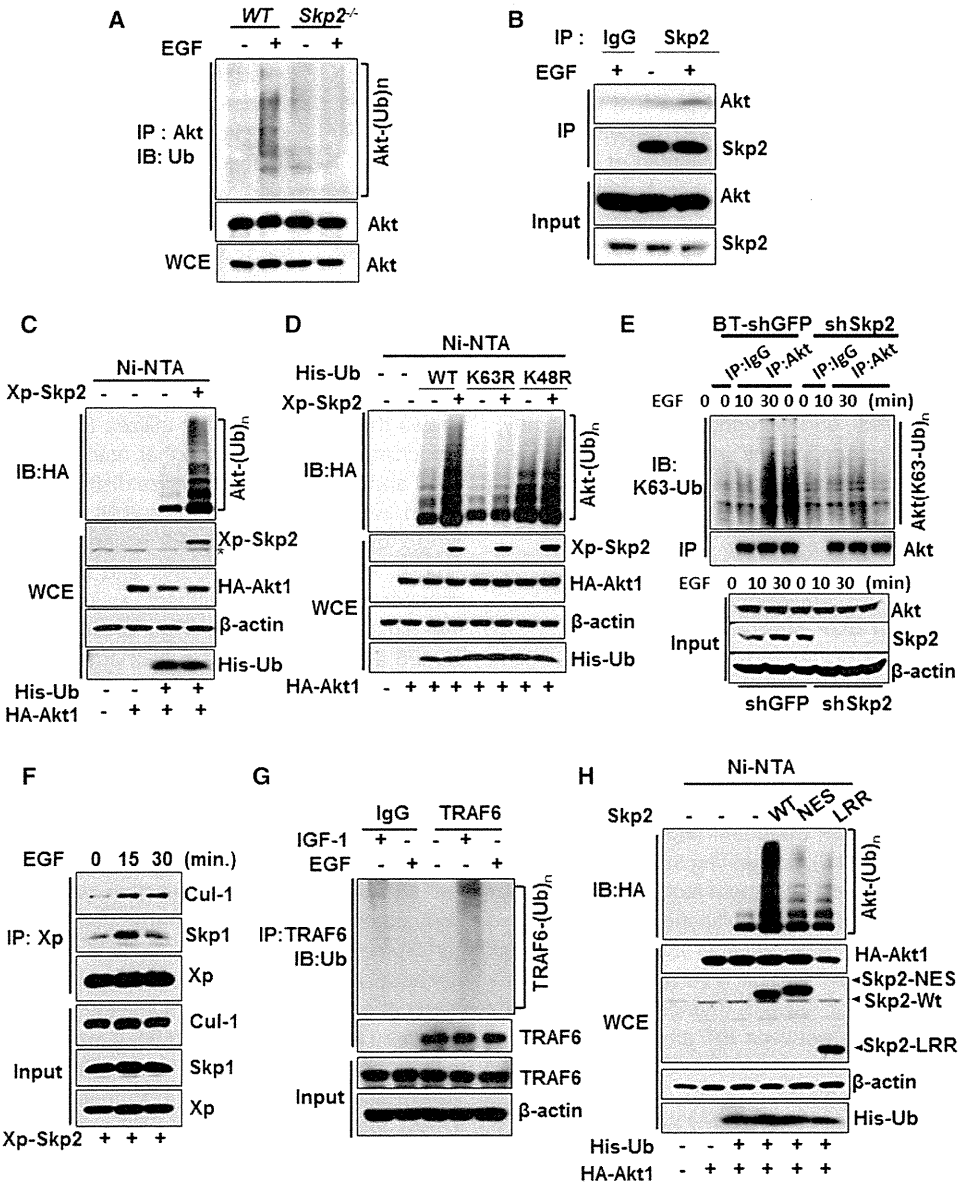

Figure 1. Skp2 Is Required for EGF-Mediated Akt Ubiquitination

(A) *WT* and *Skp2*$^{-/-}$ MEFs were serum-starved, treated with or without EGF, and harvested for in vivo ubiquitination assay.

(B) 293T cells were serum-starved, treated with or without EGF and harvested for coimmunoprecipitation (co-IP) assay followed by immunoblot (IB) analysis.

(C) In vivo ubiquitination assay in 293T cells transfected with hemagglutinin (HA)-Akt1 and His-ubiquitin (His-Ub), along with Xpress-Skp2 (Xp-Skp2). Ni-nitrilotriacetic acid (NTA) indicates nickel bead precipitate; WCE indicates whole-cell extracts. *Indicates nonspecific signal.

(D) In vivo ubiquitination assay in 293T cells transfected with various constructs.

(E) Control- and Skp2-knockdown BT-474 cells were serum-starved, treated with or without EGF, and harvested for in vivo ubiquitination assay.

(F) 293T cells were transfected with Xp-Skp2, serum-starved, treated with or without EGF, and harvested for co-IP assay followed by IB analysis.

(G) Cos1 cells were serum-starved, treated with or without IGF-1 or EGF and harvested for in vivo ubiquitination assay.

(H) In vivo ubiquitination assay in 293T cells transfected with HA-Akt1, His-Ub, along with *WT* Skp2 and E3-ligase dead mutants (Skp2-NES and Skp2-LRR).

See also Figures S1 and S2.

(Figures S2H and S2I). Collectively, these results suggest that various receptor tyrosine kinases (RTKs) can recruit, activate distinct E3 ligases and regulate the interaction between Akt and distinct E3 ligases, thereby contributing to RTK-mediated Akt ubiquitination.

The Skp2-SCF Complex Is Required for Akt Ubiquitination and Activation Triggered by ErbB Family Signaling

Whereas Skp2 overexpression promoted in vivo Akt ubiquitination, Skp2-NES and Skp2-LRR mutants, both of which have

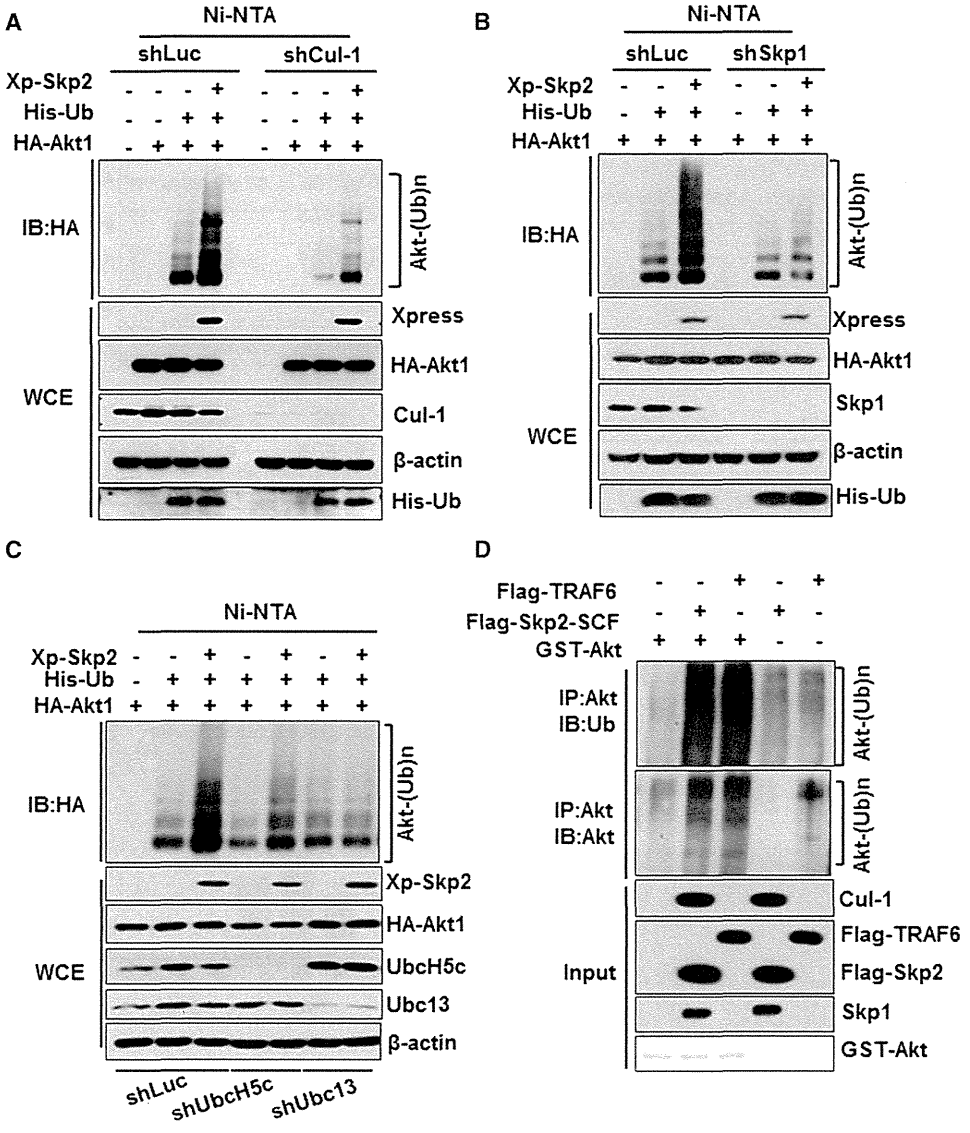

Figure 2. Skp2 SCF Complex Is a Direct E3 Ligase for Akt

(A) Luciferase or Cul-1-silenced 293 cells transfected with various constructs were harvested for in vivo ubiquitination assay.

(B) In vivo ubiquitination assay in Luciferase or Skp1-silenced 293 cells transfected with various constructs.

(C) In vivo ubiquitination assay in various 293 knockdown cells transfected with different plasmids.

(D) GST-Akt proteins were incubated with adenosine triphosphate, E1, and E2 (both UbcH5c and Ubc13/Uev1) along with or without Flag-Skp2-SCF or Flag-TRAF6 for in vitro Akt ubiquitination assay.

See also Figure S3.

defects in Skp2 SCF E3 ligase activity (Chan et al., 2010a; Kim et al., 2003; Lin et al., 2009), compromised this effect (Figure 1H). Of note, the impairment of Skp2-NES mutant in promoting Akt ubiquitination was not due to its defect in Akt binding (Figure S2J). Likewise, Skp2-mediatd in vivo Akt ubiquitination was profoundly compromised upon Cul-1 or Skp1 knockdown (Figures 2A and 2B). Interestingly, silencing both UbcH5c and Ubc13, two ubiquitin-conjugating enzymes (E2s) critical for K63-linked ubiquitination (Xia et al., 2009; Zeng et al., 2010), attenuated Skp2-mediated Akt ubiquitination (Figure 2C). We found that Skp2, but not Skp1 and Cul-1, could directly interact with Akt (Figure S3) and that Skp2 SCF complex readily triggered in vitro Akt ubiquitination, in a manner similar to that of TRAF6 (Figure 2D). Thus, Skp2 SCF complex is a direct E3 ligase for Akt.

We next determined whether Skp2 SCF complex is required for EGF-mediated Akt activation. Strikingly, EGF-induced phosphorylation of Akt and Foxo1 were markedly reduced in *Skp2*$^{-/-}$ MEFs compared to that in *WT* MEFs (Figure 3A). We observed a similar impairment in EGF-mediated Akt phosphorylation upon Skp2, Cul-1, Skp1, UbcH5c, or Ubc13 knockdown (Figures 3B and S4A–S4C). Accordingly, these results indicate that

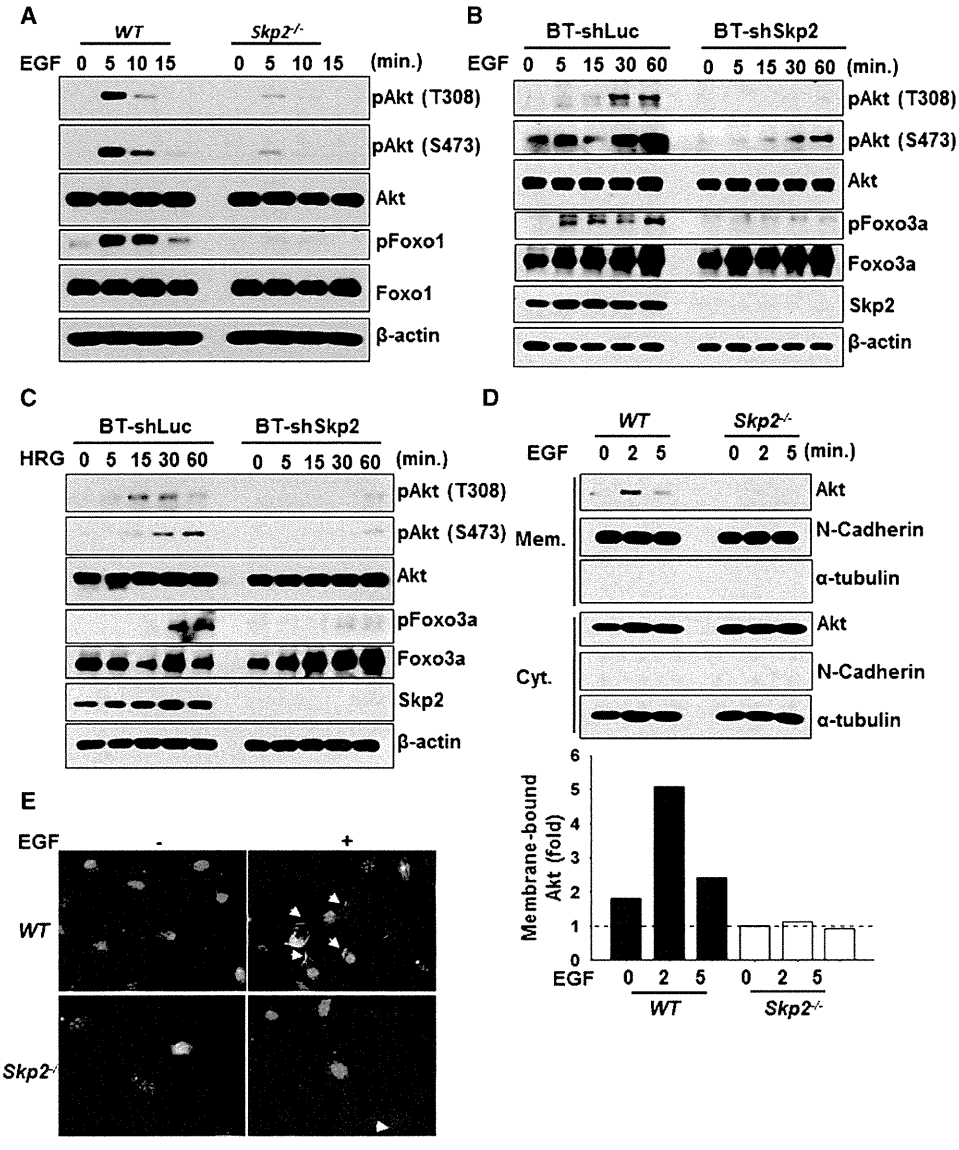

Figure 3. Skp2 SCF Complex Is Required for Akt Activation and Membrane Recruitment

(A) *WT* and *Skp2*$^{-/-}$ MEFs were serum-starved, treated with EGF for various time points and harvested for IB analysis.

(B and C) BT-474 cells with control- and Skp2-silenced were serum-starved, treated with EGF (B) or HRG (C) for various time points and harvested for IB analysis.

(D) *WT* and *Skp2*$^{-/-}$ MEFs were serum-starved, treated with EGF for various time points, and the membrane (mem) and cytosolic (cyt) fractions were isolated for IB analysis. The relative intensity of was quantified with ImageQuant software and normalized with the Akt levels in *WT* MEFs without EGF treatment.

(E) *WT* and *Skp2*$^{-/-}$ MEFs were serum-starved, treated with EGF for 5 min and fixed for immunofluorescence assay. The arrow indicates the membrane localization of Akt. The quantification results were shown in Figure S4G.

See also Figure S4.

the Skp2 SCF complex is critical for EGF-triggered Akt phosphorylation and activation. To determine whether Skp2 is also involved in Akt signaling activation by other ErbB family proteins, BT-474 breast cancer cells were treated with Heregulin (HRG), which is known to activate ErbB2 and ErbB3 (Agus et al., 2002; Lee-Hoeflich et al., 2008). Notably, Skp2 knockdown also impaired Akt phosphorylation and activation in BT-474 cells upon HRG treatment (Figure 3C). These results suggest that Skp2 is generally involved in Akt activation in response to ErbB receptor signaling.

We next examined whether Skp2 regulates the ubiquitination of other Akt isoforms. Notably, we found ubiquitination of both Akt1 and Akt2, but not Akt3 were induced by Skp2 overexpression, although basal ubiquitination of Akt2 was lower than that of Akt1 (Figure S4D). Furthermore, Skp2 deficiency attenuated EGF-mediated Akt1 and Akt2 phosphorylation (Figure S4E), indicating that Skp2 is required for EGF-promoted activation of both Akt1 and Akt2.

As TRAF6-mediated Akt ubiquitination at K8 and K14 residues is critical for its membrane recruitment and activation (Yang

et al., 2009), we then validated whether these two sites are also being utilized by Skp2 SCF complex. Indeed, we found that K8 and K14 residues are essential sites for Skp2-mediated Akt ubiquitination (Figure S4F). Biochemical fractionation assay and immunofluorescence assay revealed that EGF-induced Akt membrane recruitment was dramatically impaired in *Skp2*$^{-/-}$ MEFs compared to that in *WT* MEFs (Figures 3D and 3E and S4G).

Although the binding of Akt to PIP3 is an essential step for Akt membrane recruitment and activation, our recent report reveals that K63-linked ubiquitination of Akt plays a dispensable role in Akt and PIP3 binding (Yang et al., 2009). We further excluded the possibility that Skp2 regulates Akt membrane recruitment and activation by affecting Akt and PIP3 binding (Figure S4H). Although Akt dimerization is also proposed to be important for Akt activation (Datta et al., 1995; Künstle et al., 2002; Noguchi et al., 2007), ubiquitination-dead mutant of Akt displayed similar capability to form Akt dimer as WT Akt did (Figure S4I), suggesting that Akt ubiquitination does not regulate Akt dimerization.

Skp2 Regulates Glycolysis through Inducing Akt Ubiquitination and Activation

Cancer cells evolve to develop a mechanism that increases glucose uptake and glycolysis to generate higher ATP levels, a phenomenon called Warburg effect (Warburg, 1956). The Warburg effect is critically regulated by Akt, which is highly activated in human cancers (Elstrom et al., 2004; Manning and Cantley, 2007; Plas and Thompson, 2005; Robey and Hay, 2009). As Skp2 orchestrates Akt ubiquitination and activation, it is conceivable that Skp2 may regulate glucose uptake and glycolysis. Indeed, we found that Skp2 knockdown suppressed glucose uptake and glycolysis in breast cancer cells upon EGF or HRG stimulation, as determined by lactate production and glucose incorporation assays (Figures 4A and 4B and S5A–S5C and S5E), in a manner similar to that of PI3K/Akt inhibition (Figures 4B and 4C and S5D and S5F). To further investigate whether Skp2 regulates in vivo glycolysis and breast cancer development, we monitored the impact of Skp2 expression on in vivo glucose uptake and subsequent tumor growth in a xenograft model bearing Her2-overexpressing breast tumors. Although in vivo glucose uptake was enriched in control-silenced breast tumors, it was profoundly reduced upon Skp2 knockdown, which correlated with tumor suppression upon Skp2 silencing (Figures 4D–4G). Accordingly, Skp2 promotes in vivo glycolysis and breast cancer development.

Intriguingly, introduction of Myr-Akt, a constitutively active form of Akt, rescued the defect in lactate production of Skp2-knockdown cells in the presence of EGF or HRG (Figures 5A and S6A and S6B), suggesting that Skp2 regulates glycolysis in cancer cells through modulating Akt activation. Because Akt regulates glucose uptake by inducing gene expression and membrane translocation of Glut1 (glucose transporter type 1), a predominant glucose transporter expressed in most cell types (Barthel et al., 1999; Wieman et al., 2007), we examined whether Glut1 is a downstream target of Skp2 in regulating glycolytic phenotype. As expected, Skp2 deficiency reduced Glut1 transcription and protein expression in breast cancer cells, recapitulating the phenotype driven by Akt inactivation (Figures 5B, 5C, and 5F and S5E–S5G). Importantly, we found that Glut1 protein expression in both membrane fraction and total cell extracts was markedly induced by EGF in control-knockdown cells; however, this induction was impaired in Skp2-deficient cells (Figures 5D and 5E and S6C). The inhibition of Glut1 protein expression in Skp2-knockdown cancer cells was also rescued by the introduction of Myr-Akt (Figure 5F), underscoring that Skp2 regulates Glut1 expression through Akt activation.

To further support our notion that Skp2 regulates glycolysis through Akt ubiquitination, we introduced Akt-Wt, Myr-Akt and Akt-K8R/K14R in Skp2-deficient cells to investigate their effects on glucose metabolism. Notably, although the introduction of Akt-Wt or Myr-Akt rescued the defect in lactate production of Skp2-knockdown cells in the presence of EGF or HRG, Akt-K8R/K14R mutant failed to do so (Figures 5G and S6A and S6B). These results indicate that Skp2 controls glycolysis in cancer cells through regulating Akt ubiquitination and activation.

Skp2 Loss Attenuates Akt Activity, Glut1 Expression, and Mammary Tumor Development in *MMTV-Neu* Mice

As Skp2 is critical for ErbB receptor signaling, we examined the role of Skp2 loss in Akt activation, Glut1 expression, and tumorigenesis in *MMTV-Neu* transgenic mice, which develop primary and metastatic breast cancer (Oshima et al., 2004). Kaplan-Meier survival analysis revealed that *Skp2* deficiency significantly prolonged the survival of *MMTV-Neu* mice (Figure 6A). Notably, *Skp2* deficiency markedly delayed breast cancer development and reduced breast tumor volume in *MMTV-Neu* mice, thereby restricting breast cancer metastasizing to the lungs (Figures 6B–6E). *Skp2* loss also inhibited in vivo Akt activation and Glut1 expression in *MMTV-Neu* mice, correlated with the reduced Ki-67 expression of *MMTV-Neu* mice (Figure 6F). Collectively, *Skp2* deficiency inhibits Akt activation and Glut1 expression in vitro and in vivo, in turn repressing breast cancer development.

Skp2 Serves as a Marker for Poor Prognosis in Her2-Positive Breast Cancer Patients

Because Skp2 regulates Akt activation and tumorigenesis in *MMTV-Neu* mouse model, we next investigated whether Skp2 correlates with Akt activation and serves as a marker for poor prognosis in Her2-positive breast cancer patients. For this purpose, we have retrospectively identified 213 consecutively treated breast cancer patients that received modified radical mastectomy with curative intent and without neither pre- nor postoperative adjuvant chemotherapy and/or radiation therapy. Among them, 80 cases were Her2-positve (defined as 3+), whereas 132 were Her2-negative (defined as 0 to 2+). In these 80 cases of Her2-positive breast carcinomas, Skp2 overexpression was significantly correlated with numerous adverse clinicopathological factors, including increments of primary tumor status (pT, $p = 0.05$), nodal metastasis (pN, $p = 0.012$), and stage ($p = 0.026$) (Table S1). Skp2 expression also significantly correlated with the upregulation of pAkt (S473) ($p < 0.001$) (Figure 7A and Table S1). We next asked the question whether Skp2 expression also correlates with both Akt1 and Akt2 phosphorylation in breast tumors. Interestingly, phosphorylation of both Akt isoforms was higher in Skp2-high tumors than that in

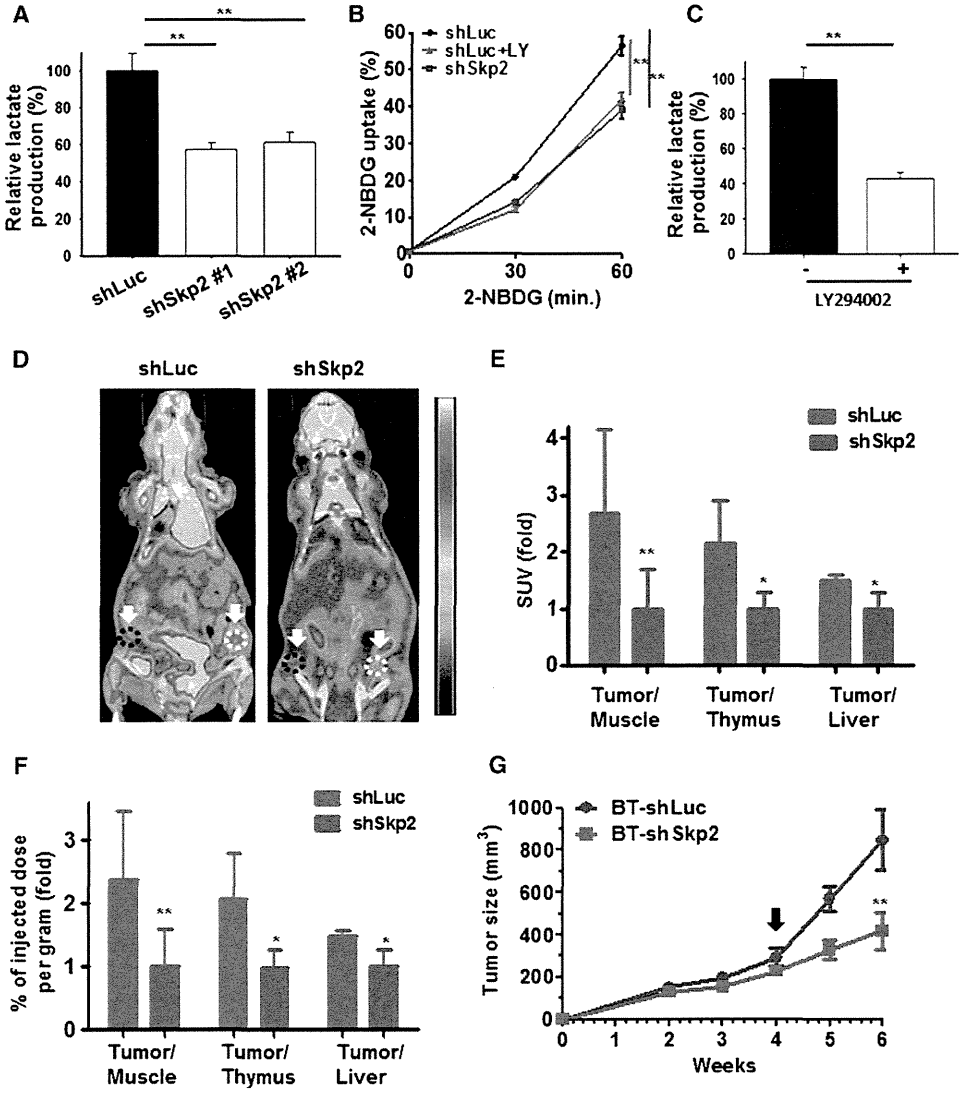

Figure 4. Skp2 Regulates Glucose Uptake and Glycolysis In Vitro and In Vivo

(A) Lactate production was measured in BT-474 cells with Luciferase and Skp2 knockdown.

(B) Glucose uptake was measured in BT-474 cells with Luciferase and Skp2 knockdown. Cells treated with or without LY294002 were grown in the presence of the fluorescent analog NBDG for various time points, and glucose uptake was quantified using FACS analysis.

(C) Lactate production was measured in BT-474 cells treated with or without LY294002.

(D) Representative PET/CT images in nude mice bearing breast tumors with luciferase- or Skp2-knockdown. White dotted lines indicate area of the breast tumors and black dotted lines indicate area of muscle tissues that were analyzed for in vivo glucose uptake.

(E and F) Glucose uptake was expressed as standard uptake value (SUV) ratio (E) or as percent of injected dose per gram (F) of labeled [^{18}F] FDG-glucose incorporation in mice bearing Luciferase- or Skp2-silenced breast tumors. Glucose uptake in breast tumors was normalized with muscle, thymus or liver tissues in each mouse. The quantified results are presented as means ± SD (n = 5).

(G) Breast tumor development in nude mice bearing breast tumors with luciferase- or Skp2-knockdown (n = 5). The arrow indicates the time point for in vivo glucose uptake analysis. **p < 0.01.

See also Figure S5.

Skp2-low tumors, and Skp2 expression nicely correlated with Her2 levels in breast tumors (Figure 7B). Our results suggest that Skp2 upregulation in Her2-positve breast tumors may contribute to activation of Akt1 and Akt2, thereby promoting breast cancer progression in Her2-positive breast cancer patients.

As Akt-mediated Skp2 S72 phosphorylation stabilizes Skp2 expression and enhances its E3 ligase activity (Gao et al., 2009; Lin et al., 2009), we asked the question whether this Akt-mediated phosphorylation of Skp2 may serve as a positive feedback loop for Akt ubiquitination. Indeed, we found that the Skp2 S72A mutant defective in Akt-mediated phosphorylation

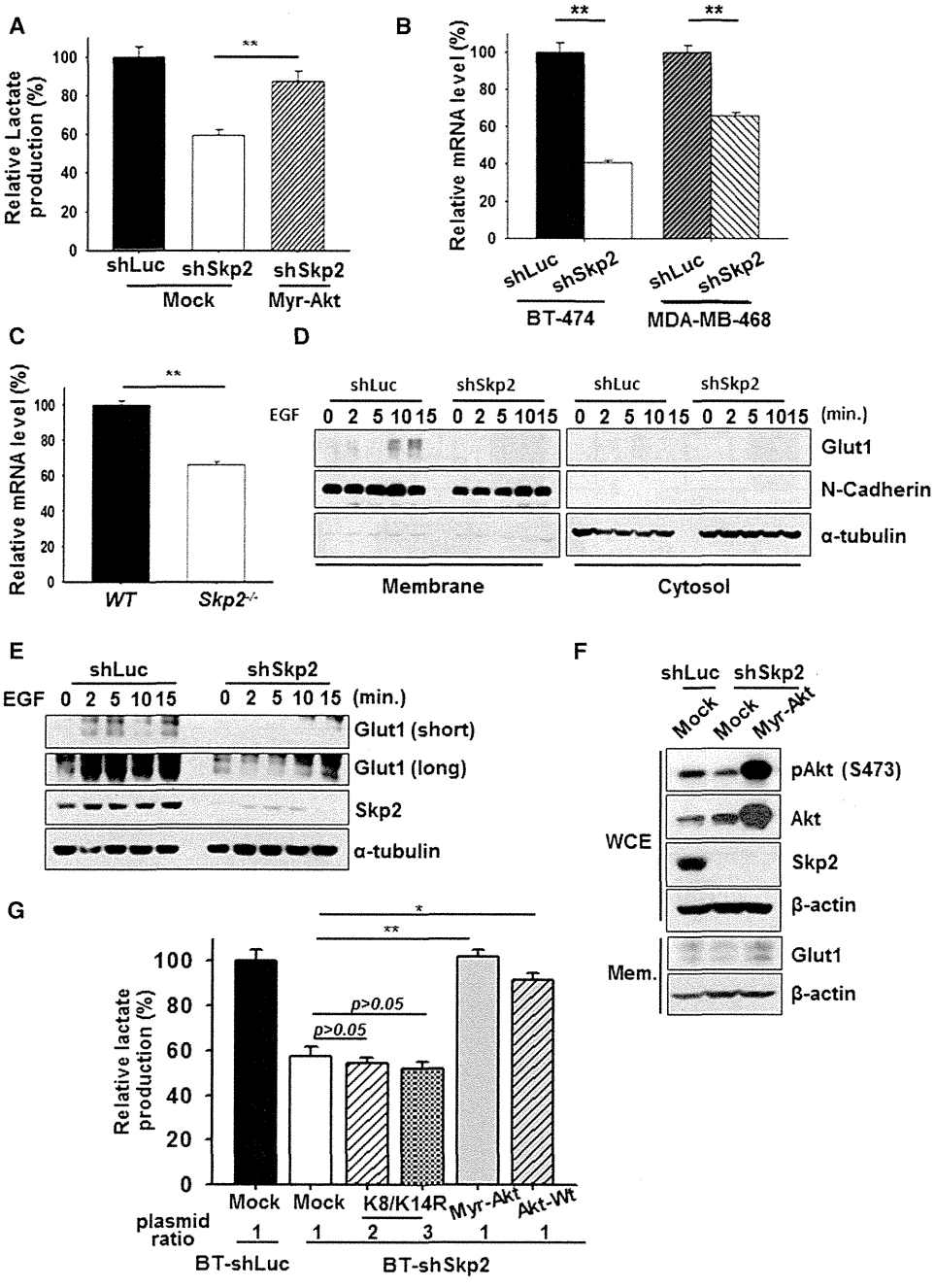

Figure 5. Skp2 Regulates Glycolysis through Promoting Akt Ubiquitination and Activation

(A) Lactate production was determined in BT-474 cells with luciferase, Skp2 knockdown, or Skp2 knockdown plus Myr-Akt overexpression upon EGF stimulation.

(B) Real-Time PCR analysis of Glut1 mRNA levels in BT-474 cells or MDA-MB-468 cells with luciferase or Skp2 knockdown.

(C) Real-Time PCR analysis of Glut1 mRNA Levels in *WT* and *Skp2*$^{-/-}$ MEFs.

(D) Cos1 cells with luciferase or Skp2 knockdown were serum-starved, treated with EGF for various time points and harvested for the isolation of membrane and cytosolic fractions, followed by IB analysis.

(E) Cos1 cells with LUCIFERASE or Skp2 knockdown were serum-starved, treated with EGF for various time points and harvested for IB analysis.

(F) IB analysis of Glut1 protein expressions in whole cell extracts (WCE) or membrane fractions (Mem) of BT-474 cells with luciferase, Skp2 knockdown, or Skp2 knockdown plus Myr-Akt overexpression.

(G) Lactate production was measured in Luciferase- and Skp2-silenced BT-474 cells transfected with various constructs as indicated upon EGF stimulation. The quantified results are presented as means ± SD (n = 3). *p < 0.05; **p < 0.01.

See also Figure S6.

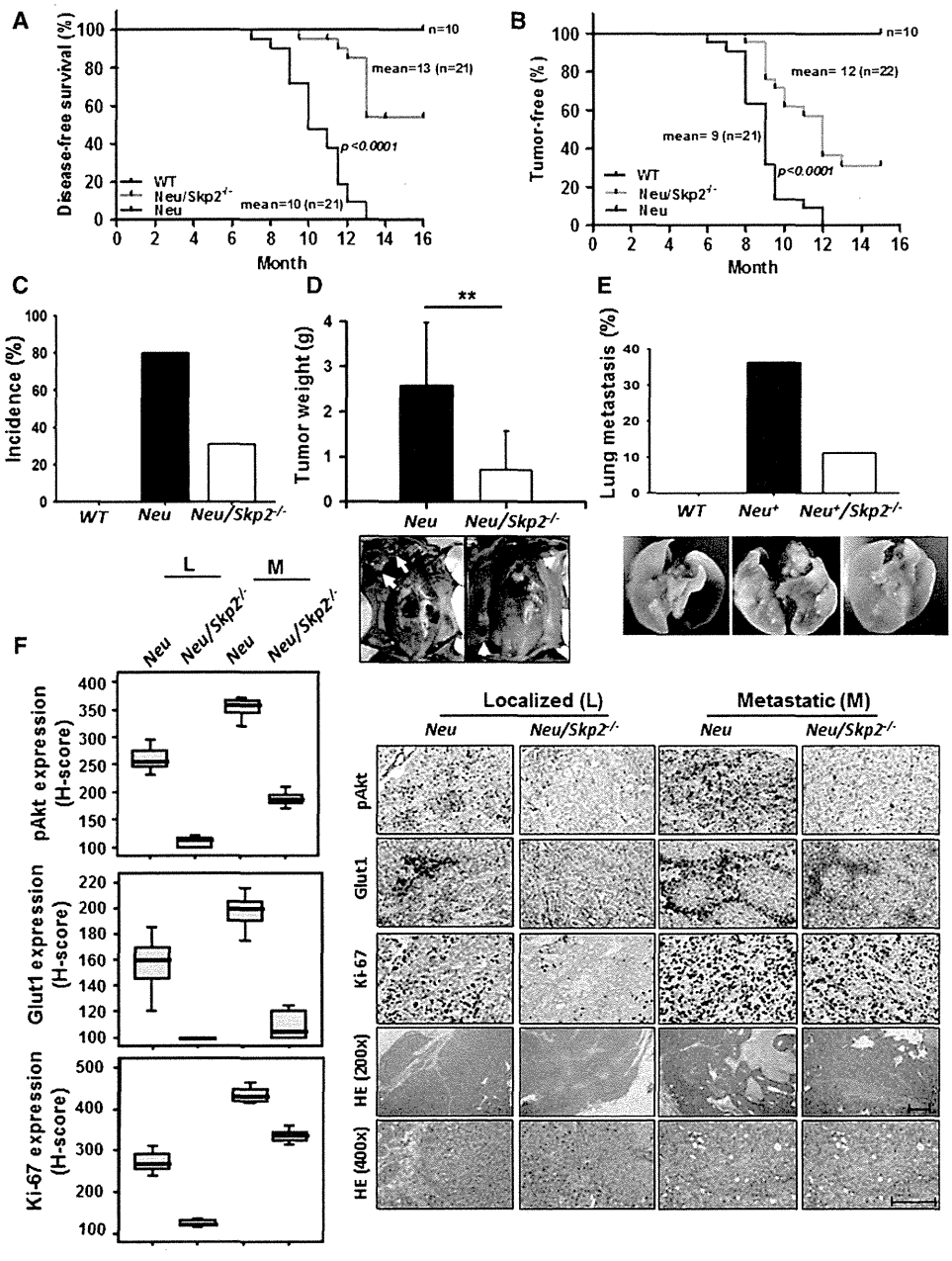

Figure 6. *Skp2* Deficiency Restricts In Vivo Akt Activation and Mammary Tumor Development upon Neu Overexpression

(A) Kaplan-Meier plot analysis of cumulative disease-free survival of *WT*, *MMTV-Neu*, and *MMTV-Neu/Skp2*$^{-/-}$ mice.

(B) Kaplan-Meier plot analysis of tumor-free incidence of *WT*, *MMTV-Neu*, and *MMTV-Neu/Skp2*$^{-/-}$ mice.

(C) The percentage of mice that develop mammary tumor was analyzed from a cohort of *WT*, *MMTV-Neu*, and *MMTV-Neu/Skp2*$^{-/-}$ mice at age around 10 months (*WT*, n = 10; *MMTV-Neu*, n = 13; *MMTV-Neu/Skp2*$^{-/-}$, n = 10).

(D) Mammary tumors were obtained and weighed from *MMTV-Neu* and *MMTV-Neu/Skp2*$^{-/-}$ mice at the age around 10 months (*MMTV-Neu*, n = 11; *MMTV-Neu/Skp2*$^{-/-}$, n = 10). The quantified results are presented as means ± SD. Arrows indicate mammary tumors. **p < 0.01.

(E) The percentage of mice that develop lung metastasis was analyzed from a cohort of *WT*, *MMTV-Neu*, and *MMTV-Neu/Skp2*$^{-/-}$ mice at age ~12 months (*WT*, n = 10; *MMTV-Neu*, n = 11; *MMTV-Neu/Skp2*$^{-/-}$, n = 9).

(F) Histological and quantification analysis of pAkt, Glut1, and Ki-67 protein expression in *MMTV-Neu* and *MMTV-Neu/Skp2*$^{-/-}$ mice. Scale bar represents 200 μm. All p value < 0.001 by using Mann-Whitney U test, except the p value for Glut1 expression between localized and metastatic *MMTV-Neu/Skp2*$^{-/-}$ (p = 0.105).

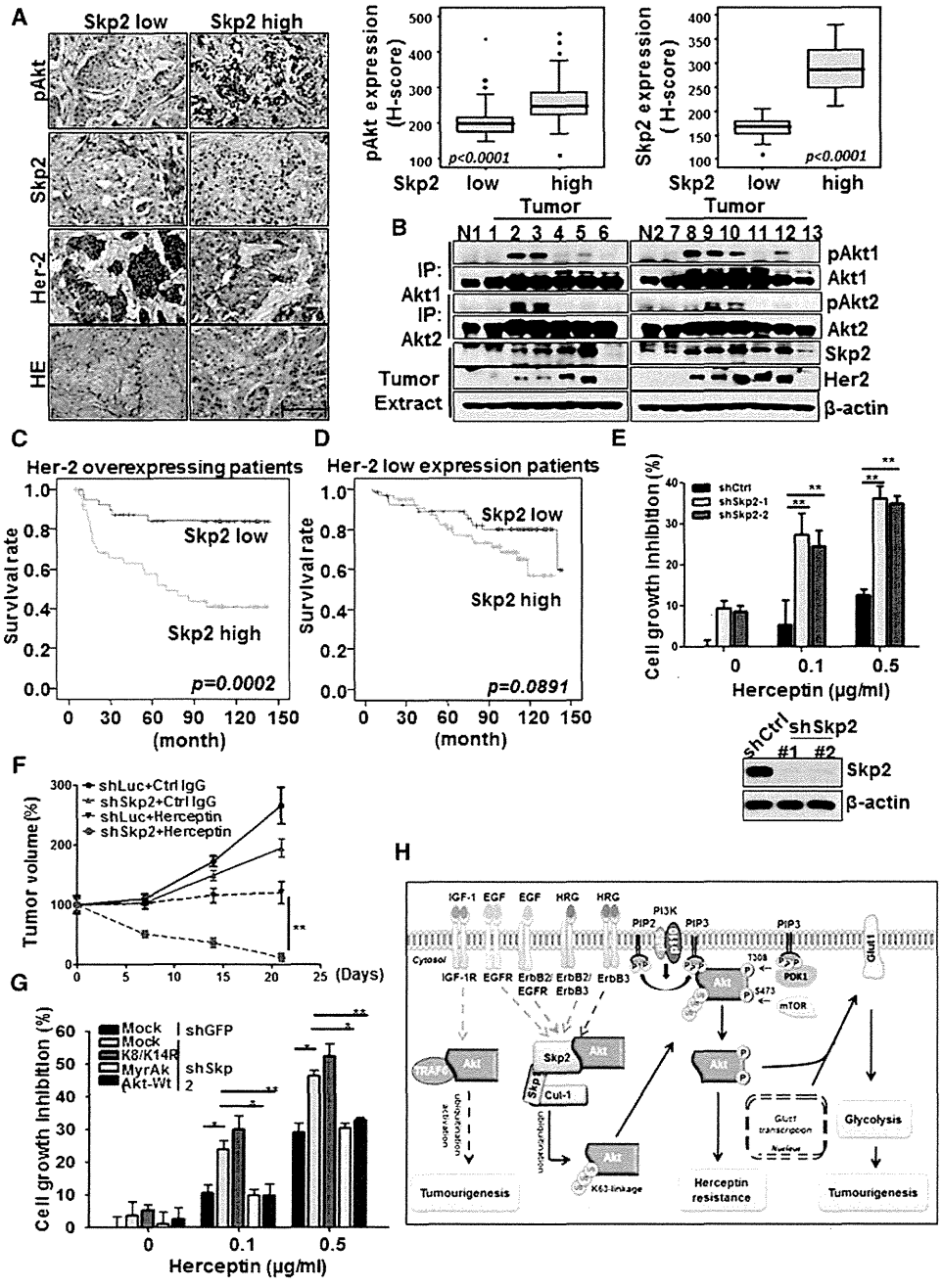

Figure 7. Skp2 Deficiency Prolongs Survival of Her2-Positve Patients and Confers Herceptin Sensitivity in Her2-Positive Cells and Tumors

(A) Histological and quantification analysis of pAkt expressions in Her2-positive patients with low or high expression of Skp2. Scale bar represents 200 μm. All p value < 0.001 by using Mann-Whitney U test.

(B) Breast tumors and normal breast tissues were extracted and subjected for IP assay, followed by IB analysis.

(C) Kaplan-Meier plot analysis of metastasis-free survival of 80 cases of Her2-positive patients with low or high expression of Skp2.

(D) Kaplan-Meier plot analysis of metastasis-free survival of 132 cases of Her2 low-expressing patients with low or high expression of Skp2.

(E) Cell growth inhibition assay and IB analysis in BT-474 cells with luciferase or Skp2 knockdown. BT-474 cells were treated with various doses of Herceptin for 6 days and cell numbers were counted using hemocytometer.

(F) Tumor volume of Her2-positive tumors with or without Skp2 silencing upon treatment with IgG or Herceptin. Tumor volume at various time points of treatment is presented as percentage of original tumor size (~200 mm^3) at day zero of treatment. The quantified results are presented as means ± SD (n = 6). **p < 0.01.

(G) BT-474 cells with luciferase or Skp2 knockdown were transfected with various plasmids, treated with various doses of Herceptin and viable cell numbers were counted using hemocytometer. The quantified results are presented as means ± SD (n = 3). *p < 0.05; **p < 0.01.

(H) The working model of Skp2 in ErbB family-regulated Akt activation, glycolysis, and tumorigenesis.

See also Figure S7 and Tables S1, S2, S3, and S4.

reduced its ability to promote Akt ubiquitination compared to WT Skp2 (Figure S7A). Moreover, we found that the Skp2-S72A mutant was defective in promoting Akt phosphorylation and activation in breast cancer cells (Figure S7B). Interestingly, the level of Skp2 S72 phosphorylation was upregulated and correlated with pAkt levels in multiple breast cancer cell lines (Figure S7C), suggesting that Skp2 phosphorylation is upregulated in breast cancer cells and correlates with Akt activation. Moreover, Skp2 S72A mutant compromised its ability to promote breast cancer cell migration and invasion compared to that of WT Skp2 (Figures S7D and S7E), correlated with its defect in promoting Akt ubiquitination and activation (Figures S7A and S7B). Future work would be required to further understand whether Skp2 phosphorylation orchestrates breast cancer metastasis.

In the univariate survival analysis, Skp2 ($p = 0.0048$ by continuous scoring) and pAkt (S473) ($p = 0.0134$) overexpression, together with pT status ($p < 0.0001$), pN status ($p = 0.0016$), and stage ($p < 0.0001$) effectively predicted inferior metastasis-free survival ($p = 0.0002$ by binary cut-offs) (Figure 7C and Table S2). In the multivariate analysis, although Skp2 overexpression remained prognostically significant for metastasis-free survival in Her2-positive breast cancer patients ($p = 0.0343$ by continuous scoring in multivariate analysis, $p = 0.0048$ by continuous scoring in univariate analysis) (Table S2), this prognostic effect was not significant in our 132 in-house Her2-negative breast cancers ($p = 0.1065$ by continuous scoring in univariate analysis and $p = 0.0891$ by binary cut-offs) (Figure 7D and Table S3). Moreover, Skp2 level did not significantly correlate with pAkt (S473) level in Her2-negative breast cancer samples ($p = 0.672$, Table S4). To further strengthen our notion that Skp2 serves as a biomarker for poor prognosis, we have analyzed the correlation between Skp2 and Her2 mRNA levels in NKI dataset (van de Vijver et al., 2002) and found that high Skp2 mRNA level significantly predicted inferior distal metastasis-free survival ($p = 0.0018$) in Her2 overexpressing breast cancer, but not in Her2 low expressing breast cancer ($p = 0.1364$) (Figures S7F and S7G). Our results collectively suggest that the status of Skp2 expression can predict survival outcome of Her2-positive breast cancer patients.

Skp2 Deficiency Enhances Herceptin Sensitivity in Her2-Positive Cancer Cells and Tumors

Herceptin is the standard treatment for Her2-positive breast tumors that substantially improves the clinical outcomes of these patients. However, there are still a number of patients that display intrinsic or acquired resistance to this treatment. The discordant Herceptin responses among Her2-positive patients are possibly due to the heterogeneous nature of tumors. As *Skp2* deficiency or knockdown inhibits glycolysis in mouse tumor models (Figures 4D–4F and 6F), we examined whether Skp2 targeting sensitizes Herceptin response in Her2-positive cancer cells and tumors. Indeed, the Herceptin sensitivity was significantly enhanced in Skp2-silenced cells (Figures 7E and S7H). In preclinical mouse model, although Herceptin by itself inhibited tumor growth, it did not cause tumor shrinkage (Figure 7F). Strikingly, Skp2 silencing in conjunction with Herceptin treatment resulted in substantial tumor regression (Figure 7F), highlighting that Skp2 is an appealing therapeutic target to combine with Herceptin for anticancer treatment.

To support the notion that Skp2 regulates Herceptin resistance through promoting Akt ubiquitination and activation, we introduced Akt-K8R/K14R, Akt-WT, and Myr-Akt in Skp2-silenced cells to examine their effects on Herceptin sensitivity. Notably, overexpression of WT Akt or Myr-Akt prevented heightened Herceptin sensitivity in Skp2-silecned cells, whereas Akt-K8/K14R overexpression failed to do so (Figure 7G), elucidating that Skp2 regulates Herceptin resistance through promoting Akt ubiquitination.

DISCUSSION

Our results reveal several unexpected findings with important clinical implications. We identify that the Skp2 SCF complex is a crucial E3 ligase for promoting Akt ubiquitination and activation, thereby resulting in elevated glycolysis and tumorigenesis in response to ErbB receptor signaling (Figure 7H). Importantly, we provide preclinical evidence demonstrating that targeting glycolysis drastically benefits therapeutic outcomes for current anticancer treatments.

Different Growth Factors Utilize Distinct E3 Ligases for Akt Ubiquitination and Activation

Our current and previous findings establish that K63-linked ubiquitination of Akt is a general event triggered by growth factors and cytokines, such as IGF-1, EGF and interleukin-1, and plays a critical role in Akt membrane recruitment and activation. Although TRAF6 is required for IGF-mediated Akt ubiquitination and activation, our current study reveals that Skp2, but not TRAF6, is selectively engaged in Akt ubiquitination and activation driven by activation of ErbB family receptors. Given that other growth factors like PDGF and FGF are known to activate Akt signaling and we also revealed that Skp2 increased association with Akt upon stimulation of PDGF, but not FGF (data not shown), it remains to be determined whether Skp2 is involved in PDGF-mediated Akt ubiquitination and activation.

Skp2 SCF Complex Regulates Nonproteolytic K63-Linked Ubiquitination

Skp2 SCF complex is known to play a critical role in cell cycle regulation and tumorigenesis by promoting ubiquitination and degradation of p27 and p21 (Chan et al., 2010b; Lin et al., 2010; Nakayama and Nakayama, 2006). We identify that Akt is a Skp2 SCF substrate, whose ubiquitination does not lead to degradation. Thus, Akt is a substrate of Skp2 SCF complex that undergoes K63-linked ubiquitination. As Skp2 and other F-box proteins are long thought to promote ubiquitination and degradation of their substrates, our current study challenges this dogma by identifying Akt as a nonproteolytic substrate for Skp2. In light of this unexpected finding, we speculate that there may be more Skp2 protein substrates undergoing nonproteolytic K63-linked ubiquitination.

Skp2 Regulates Aerobic Glycolysis, the Warburg Effect

Elevated aerobic glycolysis is a hallmark in various tumor origins, as evidenced by the wide application of PET scan in clinical

diagnosis for detecting cancer cells with actively glucose uptake (Zhu et al., 2011). Thus, identifying factors that control cancer cell glycolysis not only can advance current knowledge of how tumor cells seize glucose metabolism to acquire survival advantage, but also provide innovative approaches for cancer therapy. Our present study uncovers an unrecognized function of Skp2 in glucose metabolism. We identify Skp2 as a critical regulator for glycolysis by regulating Akt ubiquitination and activation.

Hypoxia-inducible factor-1α (HIF-1α) can activate transcription of genes encoding Glut1, Hexokinase II, Lactate dehydrogenase A (LDH-A), as well as pyruvate dehydrogenase kinase 1 (PDK1). As such, HIF-1α accumulation stimulates glucose metabolism by increasing both glucose consumption and lactate production as PDK1 inhibits conversion of pyruvate to acetyl-CoA and suppresses oxidative phosphorylation. Because activation of Akt/mTOR is known to enhance HIF-1α translation (Jiang et al., 2001; Majumder et al., 2004), it is likely that Skp2 may also upregulate HIF-1α translation and induces HIF-1-dependent glycolysis through the Akt/mTOR pathway.

In addition to the Skp2-Akt axis, we cannot rule out the possibility that Skp2 may also cooperate with other key regulators to participate in glucose metabolism or other metabolic pathways. For instance, Myc overexpression increases transcription of many metabolic enzymes, including glycolytic enzymes (Glut1 and Hexokinase II), LDH-A, and several enzymes required for nucleotide biosynthesis (DeBerardinis et al., 2008; Osthus et al., 2000; Shim et al., 1997). Because Skp2 cooperates with Myc to activate various Myc target genes involved in cell cycle transition or cell migration (Chan et al., 2010a; Kim et al., 2003; von der Lehr et al., 2003), it implies that Skp2 may participate in Myc-dependent metabolic processes through inducing the transcription of metabolic target genes. Future study will be needed to explore this possibility.

Skp2 Is a Marker for Poor Survival Outcomes and a Potential Therapeutic Target for Her2-Positive Breast Cancer

The PI3K/Akt is one of the most important oncogenic pathways activated downstream of Her2/ErB2 in cancers (Hynes and MacDonald, 2009). Our study reveals that Skp2 overexpression correlates with Akt activation and poor survival outcomes in Her2-posivtive breast cancer patients, but not in Her2-negative ones, supporting the in vivo relevance of Skp2 in ErbB family receptor-induced Akt activation and breast cancer progression. Our findings demonstrating the pronounced defect of Skp2 silencing in glucose uptake of Her2-overexpressing tumor suggests that Skp2 targeting is a promising strategy for inhibiting glycolysis and cancer (Figures 4D–4G). Because Skp2 also recognizes and promotes degradation of p27 and p21 (Bornstein et al., 2003; Nakayama et al., 2000; Nakayama and Nakayama, 2006), it is possible that downregulation of p27 or p21 may also contribute to tumor progression or poor survival outcome driven by Skp2 overexpression.

In addition to Her2/Neu overexpression, *Skp2* loss also impacts tumorigenesis driven by *Pten*, *pRB*, and *p19ARF* inactivation in various transgenic mouse models (Lin et al., 2010; Wang et al., 2010). It is possible that Skp2 silencing may globally inhibit glycolysis driven by various oncogenic insults through regulating Akt activation or other mechanisms. Our findings along with these recent reports thereby suggest that targeting glycolysis pathways can be an important therapeutic approach for cancer treatment.

Multiple genetic or epigenetic alterations have been revealed in various cancer types. Therefore, designing a strategy that universally targets fundamental features of cancer cells, such as glycolysis, may serve as a valuable anticancer approach. Several small molecules that pharmacologically inactivate glycolysis have emerged and shown promising anticancer activities as single agent or in combination with other therapeutic modalities (Pelicano et al., 2006; Vander Heiden et al., 2009). In support of this notion, our discovery reveals that Skp2 silencing as a therapeutic strategy to inactivate glycolysis can sensitize Her2-positive cells/tumors response to Herceptin (Figures 7E–7G and S7H). As such, our study provides a proof-of-principle that targeting glycolysis is a compelling therapeutic strategy as a single or a combinatory therapy for cancer treatment.

EXPERIMENTAL PROCEDURES

Mice, Cell Culture, and Reagents

MMTV-Neu and *Skp2*$^{-/-}$ mice were described (Lin et al., 2010; Nakayama et al., 2000; Oshima et al., 2004). Mouse embryonic fibroblasts (MEFs) from wild-type and *Skp2*$^{-/-}$ mice were prepared as previously described (Lin et al., 2004, 2010). All manipulations were performed under IACUC approval protocol. 293T, Cos1, BT-474, and MDA-MB-231 cells were cultured in DMEM containing 10% fetal bovine serum (FBS). $(His)_6$-ubiquitin, $(His)_6$-ubiquitin-K48R and $(His)_6$-ubiquitin-K63R, GST-Akt1, HA-Akt1 constructs was described previously (Yang et al., 2009). Skp2-LRR construct was from W. Tansey. Herceptin was a gift from Dr. M.H. Lee.

In Vivo and In Vitro Ubiquitination Assay

In vivo and in vitro ubiquitination assays were performed as described (Lin et al., 2009; Yang et al., 2009). For in vivo ubiquitination assay, 293T cells were transfected with the indicated plasmids for 48 hr and lysed by the denatured buffer (6 M guanidine-HCl, 0.1 M Na_2HPO_4/NaH_2PO_4, 10 mM imidazole). The cell extracts were then incubated with nickel beads for 3 hr, washed, and subjected to immunoblotting analysis. For in vitro ubiquitination assays, recombinant GST and GST-Akt proteins were purified from the bacterial lysates of BL21 competent cells. Flag-Skp2 SCF complex and Flag-TRAF6 were expressed in 293T cells, immunoprecipitated by anti-Flag antibody, and eluted from Protein A/G beads using Flag peptides according to manufacturers' standard procedures. Purified GST, GST-Akt, Flag-SCF, and Flag-TRAF6 proteins were incubated for 3 hr at 37°C in 20 μl of reaction buffer (20 mM HEPES [pH 7.4], 10 mM $MgCl_2$, 1 mM DTT, 59 μM ubiquitin, 50 nM E1, 850 nM of Ubc13/Uev1a, 1 mM ATP, 30 μM creatine phosphate, and 1 U of creatine kinase). After incubation, protein mixtures were diluted in RIPA buffer and the supernatant fluid was precleared with Protein A/G beads for 1 hr, and immunoprecipitated overnight with anti-Flag antibody, after which Protein A/G beads were added for an additional 1 hr. Beads were washed four times with E1A Buffer. Proteins were eluted in SDS-sample buffer and subjected to immunoblotting analysis. All animal experiments were performed under IACUC approval protocol.

Glucose Uptake Assay

Cells were seeded in 60 mm plates. Twenty-four hours later, cells were refreshed with serum-starved (0.1% FBS) and glucose-free DMEM. Sixteen hours later, cells treated with or without 10 μM LY294002 were grown in the presence of 50 μM 2-NBDG for 30 min and 60 min, respectively, and glucose uptake was quantified using FACS analysis.